

Multimodal Large Language Models as Image Classifiers

Nikita Kisel Illia Volkov Klara Janouskova* Jiri Matas

Visual Recognition Group, Czech Technical University in Prague

kiselnik@fel.cvut.cz, volkoill@cvut.cz, janoukl1@fel.cvut.cz, matas@fel.cvut.cz

*Corresponding author

Abstract

Multimodal Large Language Model (MLLM) classification performance depends critically on evaluation protocol and ground truth quality. Studies comparing MLLMs with supervised and vision-language models report conflicting conclusions, and we show these conflicts stem from protocols that either inflate or underestimate performance. Across the most common evaluation protocols, we identify and fix key issues: model outputs that fall outside the provided class list and are discarded, inflated results from weak multiple-choice distractors, and an open-world setting that underperforms only due to poor output mapping. We additionally quantify the impact of commonly overlooked design choices — batch size, image ordering, and text encoder selection — showing they substantially affect accuracy.

Evaluating on ReGT, our multilabel reannotation of 625 ImageNet-1k classes, reveals that MLLMs benefit most from corrected labels (up to +10.8%), substantially narrowing the perceived gap with supervised models. Much of the reported MLLM underperformance on classification is thus an artifact of noisy ground truth and flawed evaluation protocol rather than genuine model deficiency. Models less reliant on supervised training signals prove most sensitive to annotation quality. Finally, we show that MLLMs can assist human annotators: in a controlled case study, annotators confirmed or integrated MLLM predictions in approximately 50% of difficult cases, demonstrating their potential for large-scale dataset curation. This work is part of the Aiming for Perfect ImageNet-1k project, see <https://klarajanouskova.github.io/ImageNet/>.

1. Introduction

Multimodal Large Language Models (MLLMs) [1, 2, 6, 8, 9, 20, 26, 27], a recent extension of Large Language Models (LLMs) [4, 11, 28, 30] into the visual domain, are capable of performing complex vision-language reasoning that integrates linguistic understanding with visual percep-



ReGT: T-shirt; sunglasses; bubble
ImGT: sunglasses
ChatGPT-4o: scuba diver
Qwen3-VL: scuba diver
SigLIP 2 giant: scuba diver
DINOv3: snorkel
EfficientNetV2: sunglasses
EfficientNet-L2: snorkel
EVA-02: snorkel



ReGT: suspension bridge; mountain
ImGT: suspension bridge
ChatGPT-4o: steel arch bridge
Qwen3-VL: suspension bridge
SigLIP 2 giant: suspension bridge
DINOv3: viaduct
EfficientNetV2: pier
EfficientNet-L2: pier
EVA-02: pier

Figure 1. Challenging visual recognition cases from ImageNet-1k. ImGT: original single ImageNet label, ReGT: our reannotations. Predictions of representative models, including DINOv3, EfficientNetV2, EfficientNet-L2, EVA-02 (self-)supervised on ImageNet, are often **wrong** on such data. Correct predictions in **green**.

tion. MLLMs performance has been extensively benchmarked [13, 17, 22, 23], primarily assessing high-level multimodal reasoning and instruction following through multiple-choice question answering. MLLMs exhibit remarkable generalization and are increasingly used by both researchers and the general public. Use-cases range from safety-critical ones such as medical diagnostics [5, 19, 37] and dangerous species classification [12], to helping with mundane office work [15, 42].

Classification performance provides a natural basis for comparing MLLMs with established computer vision methods, both supervised and Vision-Language Models (VLMs) (CLIP [29], SigLIP [35, 44]). Recent works have begun to explore this comparison [21, 40, 45]. However, depending on the evaluation protocol and task formulation, studies report conflicting conclusions: while some find that MLLMs perform substantially worse than classical vision models [45], others suggest performance comparable to

VLMs [7, 21].

MLLMs produce free-form outputs, whereas image classification requires selecting a label from a predefined class set, so model outputs must be mapped to these classes. In the literature, this mapping has been achieved by formulating MLLM classification as one of the following tasks – Open-World (OW) [7, 45], Multiple-Choice (MC) question answering [21] and Closed-World (CW) [40, 45].

Open-World (OW) is closest to everyday MLLM use: the model generates a free-form image description, which is then mapped to dataset classes, either through simple heuristics (*i.e.*, text inclusion) [7, 45] or nearest-neighbor search in a text-embedding space [7]. Following Conti *et al.*, who found embedding-based mapping to be the most effective, we adopt this strategy and further show that OW outperforms CW for half of the evaluated models. This contradicts prior work [45], which relied on string matching, indicating that previous OW limitations were due to the mapping method rather than the task itself.

Multiple-choice (MC) question answering is commonly used to benchmark MLLMs and is therefore often adopted for classification evaluation. The model selects from a set of candidate class names (up to 26 in prior work), including exactly one ground-truth label and several distractors. Distractors are sampled per-image, ranging from random to more challenging alternatives semantically close to the ground-truth label. Prior work reported that harder distractors cause only a “slight decrease” in performance [21]. We find this does not hold for newer models, where our confidence-interval-backed experiments show a larger drop under their sampling strategy. We also propose a distractor sampling method that further increases task difficulty. Yet, MC evaluation still inflates performance compared to other tasks, yielding an overly optimistic view of model ability.

The Closed-World (CW) task is designed to mimic classification with supervised models and VLMs. The model is prompted with candidate classes, ideally covering the full set of dataset classes. However, such a full-class formulation has been avoided due to input token limitations of older models [21, 45]; in our work, we are the first to use the full set of classes. As the number of candidate classes increases, out-of-prompt (OOP) predictions become more frequent, where the model generates a label that is not contained in the provided candidate list despite explicit instructions to select from it. While OOP predictions are theoretically possible in MC, they are not observed in practice due to the small number of candidates. In the literature, CW is typically avoided in favor of MC [21]; when it is used, OOP predictions are counted as incorrect [45]. We introduce CW+, which resolves OOP predictions by adopting the embedding-space nearest neighbour mapping from OW. With this approach, the main reason for avoiding CW is removed, making MC unnecessary unless the model is

constrained by input token length.

Even the best evaluation protocol is only as good as its ground truth. ImageNet-1k has long served as a foundation for pretraining and evaluating model performance. Thanks to its widespread adoption, its limitations are well-documented [3, 16, 25, 32, 36, 38, 43]. They go beyond simple image label errors ($\sim 20\%$ error rate in validation set [25]), including 15–21% of validation images containing multiple objects from different classes [3], making single-label evaluation unreliable, overlapping class definitions [38], distribution shifts between training and validation sets [16], and duplicate images [38]. Despite these limitations, ImageNet remains the de facto standard for evaluating visual recognition systems, including MLLMs [21, 40, 45].

We reannotate a substantial portion of the ImageNet-1k validation set (625 classes), mainly excluding challenging fine-grained animal categories that require extensive domain knowledge, greatly reducing annotation noise, ambiguities and other imperfections mentioned. The new labels, ReGT, are not yet public and thus unseen by any current model which enables controlled analysis of how supervised, self-supervised vision–language, and instruction-tuned MLLMs respond to improved ground truth.

The gap between top-performing MLLMs and supervised models is almost halved on the new labels. ReGT also partitions images into label categories based on agreement and multiplicity with ImGT—the original ImageNet-1k ground truth. Although supervised models remain strongest on average, self-supervised VLMs and MLLMs outperform them on images where ReGT disagrees with ImGT.

In our work we benchmark five MLLMs — the closed-source GPT-4o [27] and the open-source Qwen3-VL [41], LLaVA-OneVision [18], InternVL3.5 [6], and PaliGemma 2 [33] on the reannotated data. We also conduct preliminary experiments to study prompt design, reproducibility, encoder selection for CW+ and OW, and the influence of batch size and image order.

In a focused case study on the subset where ChatGPT disagreed with our ReGT, we conducted a second annotation pass in which annotators reviewed each image alongside anonymized predictions from GPT-4o, SigLIP 2, ImGT, and ReGT. For roughly half of these disputed cases with single-label, annotators either fully replaced or augmented the labels with GPT-4o’s predictions, revealing substantial residual label noise even after an initial careful re-annotation. This demonstrates that MLLMs can serve as powerful annotation assistants.

To assess performance on fine-grained biological categories excluded from reannotation, we additionally evaluate on the expert-curated weasel-family subset from [16].

The main contributions are:

1. **Improved MLLM Image Classification Benchmark.**

We systematically evaluate five MLLMs on ImageNet-

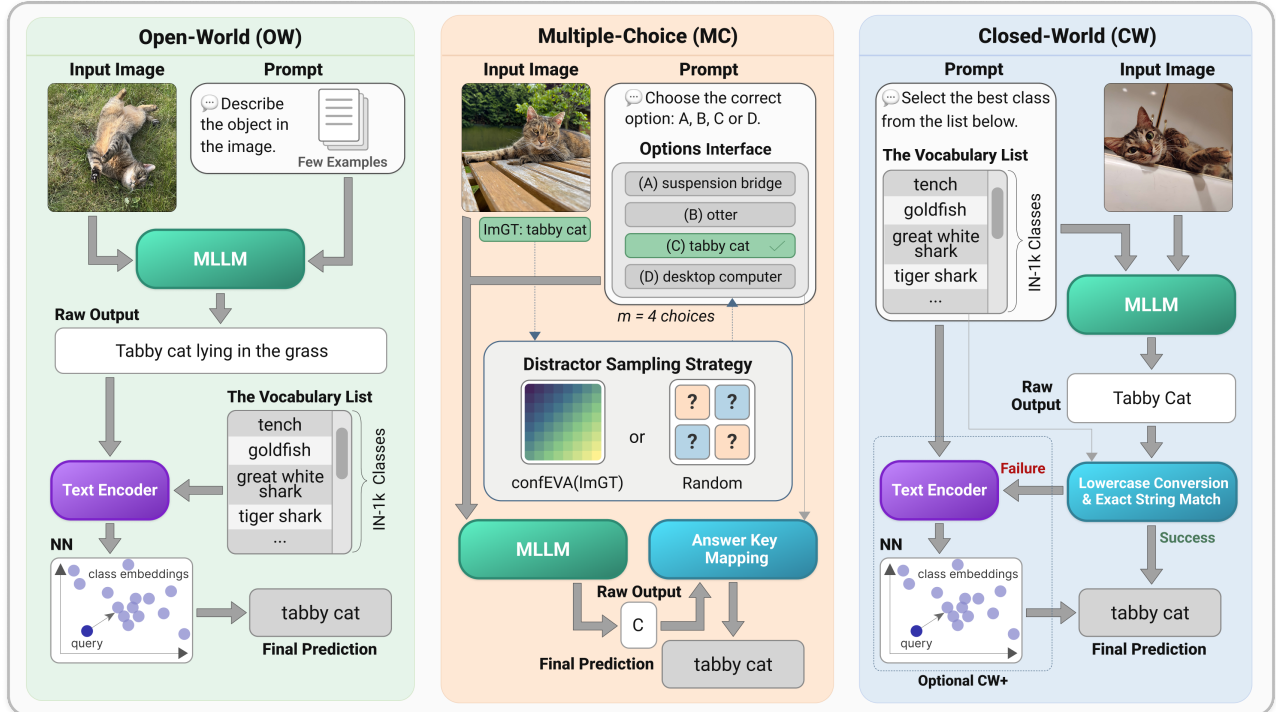


Figure 2. The three evaluated classification tasks — OW, MC, and CW(+) — described in Sec. 2.3

1k across Closed-World, Open-World, and Multiple-Choice setups within a single framework, enabling direct comparison with vision-language and supervised baselines. We introduce CW+, a lightweight embedding-based post-processing that resolves out-of-prompt predictions without costly constrained decoding, enabling full 1,000-class Closed-World evaluation. To support fair assessment, we provide a new multilabel reannotation (ReGT) of 625 classes that holistically addresses known ImageNet labeling issues.

- Label Noise Sensitivity Across Learning Paradigms.** Leveraging ReGT, we show that MLLMs benefit most from corrected labels (up to +10.8%), substantially narrowing the perceived performance gap with supervised models. This reveals that much of the reported MLLM weakness on classification is an artifact of noisy ground truth rather than genuine model deficiency, and that models less reliant on supervised training signals are more sensitive to annotation quality.
- Evaluation Protocol Sensitivity.** We quantify the impact of commonly overlooked design choices—distractor selection, batch size, image ordering, output format, and text encoder—showing that they substantially affect reported accuracy (e.g. confusion-matrix distractors cause a 10–15% drop over random ones), calling into question prior results obtained under

inflated conditions.

- MLLMs as Annotation Assistants.** In a controlled case study, human annotators confirmed or integrated the MLLM prediction in approximately 50% of difficult cases, demonstrating that MLLMs can effectively flag residual annotation errors and assist large-scale dataset curation.

2. Evaluation setup

2.1. Dataset and labels

All experiments are conducted on the ImageNet-1k dataset. Several prior works reannotated portions or even the entire validation set [3, 25, 36, 43]. However, each of these efforts addressed only a subset of the problems [16].

We introduce reannotated labels (ReGT) for 625 classes, holistically addressing known issues. We excluded fine-grained wildlife categories (except for dog breeds and species easily distinguishable without expert domain knowledge), as prior work [16, 24] showed them to be extremely challenging to annotate. To mitigate selection bias, we additionally evaluate on expert-provided *Mustelidae* reannotations [16] in the Supplementary.

Annotators, trained to recognize and avoid common issues, were asked to label all objects from ImageNet-1k classes (or indicate that none is present). To make it eas-

Cat.	Definition	Cat.	Definition
A	$N \cup S \cup M$	S^+	$S \cap \{i : gt_i \in L_i\}$
N	$\{i : L_i = 0\}$	S^-	$S \cap \{i : gt_i \notin L_i\}$
S	$\{i : L_i = 1\}$	M^+	$M \cap \{i : gt_i \in L_i\}$
M	$\{i : L_i > 1\}$	M^-	$M \cap \{i : gt_i \notin L_i\}$

Table 1. Definitions of ImageNet-1k label categories based on ReGT and ImGT differences. For image i , gt_i is the ImGT label, and L_i the set of ReGT labels. A, S, M correspond to all, single-label, and multi-label respectively, +/- denotes agreement/disagreement of ReGT and ImGT.

	A	S	S+	S-	M	M+	M-	N
#	31,250	18,071	16,177	1,894	11,834	10,756	1,078	1,345
%	100	57.8	51.8	6.1	37.9	34.4	3.5	4.3

Table 2. The number of images in each label category (#) and their fraction among reannotated images (%). Images with multiple labels (M) account for roughly 40% of image in the selected 625 classes. Approximately 5% of the images have no correct corresponding ImageNet-1k label (N).

ier to remember all classes, the annotation tool displayed top-20 model predictions for each image. While potentially introducing bias, this prevented many label omissions found in the original labels. The annotators collaborated via group chat to discuss and refine unclear class definitions or challenging individual cases.

Label categories. The categorization of images based on the number of labels in ReGT and agreement with ImGT is provided in Tab. 1.

2.2. Evaluation metric

For evaluation on ReGT, we adapt the top-1 ReaL accuracy [3]. In ReaL, a prediction is counted as correct if it matches any of an image ground-truth labels, making it suitable for multilabel images. We treat predictions on images in N (those without any valid ground-truth label) as correct, since no meaningful label supervision exists for them. We also account for semantically equivalent classes¹ (e.g. “notebook computer” vs. “laptop”), a known issue in ImageNet [16, 38]. We treat each pair in a predefined equivalence set E as interchangeable, marking a prediction correct if it matches any label in the corresponding equivalence group. This applies to both ImGT and ReGT. Formally, for the image i we define a set of admissible labels:

$$L_i^* = L_i \cup \{b \mid \exists a \in L_i, \{a, b\} \in E\}. \quad (1)$$

¹Full list is in the Supplementary

Then, the accuracy over a set of images I is

$$\text{Acc} = \frac{1}{|I|} \sum_{i \in I} \alpha_i, \quad \alpha_i = \begin{cases} 1, & p_i \in L_i^* \text{ or } |L_i| = 0, \\ 0, & \text{otherwise,} \end{cases} \quad (2)$$

where p_i is the prediction for image i .

2.3. Tasks

Task 1: Open-World (OW). The model is asked to classify the image without any predefined set of categories. A few prediction examples are given in the prompt to define the desired level of granularity. The predicted output is then embedded via a text encoder and matched with the nearest embedded class name to give the final prediction.²

Task 2: Multiple-Choice (MC). The prompt specifies n choices for each image and the model is asked to select one as the output. The choices always contain 1 correct answer and $n - 1$ distractor answers. This task can be considered a special case of Task 1 with only a subset of the classes used, but the prompt is also different. We adopt the standard [13, 17, 22, 23] $n = 4$ in all experiments. We explore multiple variants, differing in the distractor sampling strategy. The 4 options always include either the original ImGT, the ReGT, or both. The distractors can be selected at *random*, or based on the confusion matrix of the supervised EVA-02 model, denoted as $\text{confEVA}(c)$, to favour classes that are likely to be confused with the class c . It is ensured that the ImGT label distractors do not include any ReGT image labels. The evaluation is performed multiple times, each time varying the choices order and the *random* distractors.

Task 3: Closed-World (CW). The prompt provides an exhaustive list of all 1000 dataset classes and the model is asked to output a single one from the list. Since many objects may be present in the image, the model is asked to select only one class name that best describes the main object. Both the prediction and the class names are converted to lowercase; if they do not match, the prediction is considered incorrect.

2.4. Model and class names overview

Evaluated models. We evaluate five MLLMs: closed-source GPT-4o [27] and open-source Qwen3-VL [41], LLaVA-OneVision [18], InternVL3.5 [6], and PaliGemma 2 [33]. GPT-4o was selected instead of the more recent GPT-5 model due to ongoing API issues that currently make reliable evaluation difficult. Qwen3-VL was chosen as a representative leading open-source MLLM, while LLaVA-OneVision, InternVL3.5, and PaliGemma 2 cover a broader range of open-source architectures (see Tab. 3 for details). For the CW experiment, we additionally evaluate two families of VLMs: SigLIP so400M/14-384 [44] and SigLIP 2 in two sizes (so400M/16-384

²Prompts for all Tasks are available in the Supplementary.

Model	Vision Backbone	Lang. Encoder	Training Strategy
PaliGemma2-mix-28B/448	SigLIP so400M	Gemma2 27B	Joint multimodal pretraining + finetuning
LLaVA-OneVision-72B-Chat	SigLIP so400M	Qwen2 72B	Projector-based alignment + supervised finetuning
InternVL3.5-38B	InternViT 6B	Qwen3 32B	Progressive multimodal scaling + instruction tuning
Qwen3-VL-235B-A22B-Inst	SigLIP 2 so400M	Qwen3 MoE	Large-scale multimodal pretraining + instruction tuning
GPT-4o-2024-08-06	(undisclosed)	(undisclosed)	Proprietary multimodal pretraining + post-training alignment (RLHF)

Table 3. Vision backbones and language models for all five evaluated MLLMs. GPT-4o-2024-08-06 is a closed-source model; architectural details are not publicly disclosed. SigLIP-so400M denotes the shape-optimized Vision Transformer. InternViT-6B is a vanilla ViT with 6 billion parameters optimized for MLLM tasks.

Model	Task	ImGT			ReGT					Im \cap Re
		A ₃₁₂₅₀	A ₃₁₂₅₀	S ₁₈₀₇₁	S ₊₁₆₁₇₇	S ₋₁₈₉₄	M ₁₁₈₃₄	M ₊₁₀₇₅₆	M ₋₁₀₇₈	
PaliGemma2-mix-28B/448	OW	37.11 (13)	47.94 +10.8, (13)	39.74 (13)	41.49 (13)	24.76 (13)	54.55 (13)	56.24 (13)	37.66 (5)	35.78
LLaVA-OneVision-72B-Chat	OW	62.00 (12)	70.58 +8.6, (12)	67.11 (12)	70.67 (12)	36.69 (4)	72.52 (12)	75.87 (12)	39.05 (3)	59.39
InternVL3.5-38B	CW+	64.31 (11)	72.57 +8.3, (11)	67.69 (11)	71.05 (11)	39.02 (1)	76.91 (11)	80.43 (11)	41.74 (1)	61.53
Qwen3-VL-235B-A22B-Inst	OW	68.74 (10)	76.68 +7.9, (10)	73.61 (10)	77.79 (10)	37.91 (3)	78.71 (10)	82.46 (10)	41.28 (2)	65.87
GPT-4o-2024-08-06	CW+	76.40 (9)	82.36 +6.0, (9)	81.11 (9)	86.12 (9)	38.28 (2)	82.27 (9)	86.74 (9)	37.66 (5)	72.79
DINOv3 ViT-L/16 (dino.txt)	CW	80.96 (8)	85.02 +4.1, (8)	84.57 (8)	90.26 (8)	36.01 (6)	84.00 (7)	88.69 (8)	37.29 (6)	76.79
SigLIP so400M/14-384	CW	82.40 (7)	86.45 +4.0, (6)	85.59 (7)	91.35 (7)	36.38 (5)	86.23 (5)	90.96 (6)	38.96 (4)	78.27
SigLIP 2 so400M/16-384	CW	83.30 (6)	86.83 +3.5, (4)	86.06 (4)	91.99 (6)	35.32 (7)	86.52 (4)	91.47 (5)	37.20 (7)	78.93
SigLIP 2 ViT/g-opt-384	CW	84.14 (4)	87.12 +3.0, (3)	86.40 (3)	92.55 (4)	33.90 (8)	86.75 (3)	91.88 (3)	35.53 (8)	79.61
DINOv3 ViT-7B $k=11$	CW	84.18 (5)	85.61 +1.4, (7)	85.63 (6)	92.48 (5)	27.14 (11)	83.95 (8)	89.29 (7)	30.71 (11)	79.07
EfficientNetV2-XL	CW	85.28 (3)	86.53 +1.3, (5)	85.96 (5)	92.67 (3)	28.56 (9)	85.88 (6)	91.74 (4)	27.37 (12)	80.07
EfficientNet-L2	CW	88.17 (2)	88.91 +0.7, (2)	87.94 (2)	95.05 (2)	27.24 (10)	89.12 (2)	94.77 (2)	32.75 (9)	82.69
EVA-02 ViT-L-14-448	CW	90.13 (1)	90.04 -0.1, (1)	89.08 (1)	96.37 (1)	26.82 (12)	90.38 (1)	96.35 (1)	30.80 (10)	84.37

Table 4. Recognition accuracy on label categories of ImageNet-1k defined in Tab. 1 for MLLMs (top), VLMs (middle) and supervised (bottom) models. The highest-performing task (OW/CW+) is selected for the MLLMs. Increase or decrease in classification accuracy on reannotated labels w.r.t. the original labels. Model (rank)s are also shown. All models achieve higher accuracy on single-label images. The more dependence there is on the training data, the less the model benefits from the reannotation. The Im \cap Re column reports the intersection of the two correctness sets: images on which the model is correct under the ImGT and images on which it is correct under the ReGT. This value indicates the overlap between these two correctness subsets, which are otherwise largely different.

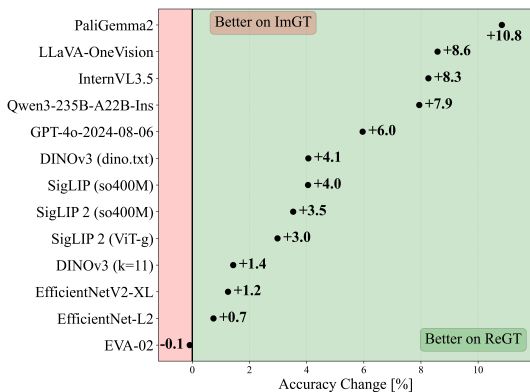


Figure 3. Classification accuracy on ImageNet-1k, change from the original (ImGT) to reannotated labels (ReGT).

and ViT/g-opt-384) [35]; DINOv3 as a zero-shot text-guided classifier ‘dino.txt’ (ViT-L/16) and as a k -NN classifier using ImageNet-1k training set (ViT-7B, $k=11$); and

Model	A	S	S+	S-	M	M+	M-	N
InternVL3.5	0.9	0.8	0.8	0.8	0.8	0.7	1.2	2.5
GPT-4o	5.3	4.0	3.4	8.7	6.0	5.6	9.9	16.4
Qwen3-VL	10.5	9.3	8.7	13.8	10.9	10.6	14.8	24.2
LLaVA-OV	26.8	24.1	23.6	28.1	29.0	28.8	31.2	42.5

Table 5. MLLMs out-of-prompt (OOP) rate, the (%) of cases when the output is none of the classes specified, per label categories. Models hallucinate more on 1. multilabel images than single label ones, 2. images that do not contain their ImGT in ReGT (S- and M-), 3. images from N category (contain no ImageNet labels in ReGT). On the last, the hallucination rate is highest for all models.

the supervised classifiers EfficientNet-L2 (trained to be robust to label noise), EfficientNetV2-XL [34] (trained on ImageNet21k), and transformer-based EVA-02 (best-performing model on ImageNet-1k according to the Timm leaderboard [39]).

Text encoder. Text-embeddings (required for OW and CW+) are computed using the best model-specific text en-



Figure 4. To address MLLMs out-of-prompt (OOP) predictions, often referred to as *hallucinations* [21, 45], we map model outputs that fall outside the provided class list to the nearest in-prompt class using the best model-specific encoder. Examples where the mapping is correct are shown. Columns correspond to the label categories from which the images were sampled. The row shows Qwen3-VL predictions, for which 38.75% OOP predictions are correctly mapped. “OOP” denotes an out-of-prompt prediction, “Map” indicates the mapped prediction, “ReGT” refers to reannotation of the image, and “ImGT” represents the original ImageNet label. Green and red stands for correct / incorrect image label.

coder in the main text. The standard mean over multiple prompt templates is used following [29]. Ablation results for alternative encoders are provided in the Supplementary in Tab. 18.

Class names. For CW and MC, we adopt the set of hand-crafted ImageNet-1k class names introduced in Kisel et al. [16]. Although we find that they contain imperfections, these are the most up-to-date version available for the dataset. It is possible to learn “optimal” class representations [46, 47] and thereby increase accuracy, but this approach would no longer be zero-shot, which contradicts the goal of our MLLMs classification evaluation.

3. Results

We compare MLLMs, VLMs, and vision-only architectures on ImageNet-1k with ImGT and ReGT. The results reveal differences in robustness and label dependence, with reannotation reducing the performance gap and an embedding-based mapping further mitigating hallucination errors.

Preliminary experiments results. The impact of batch size, image ordering within a batch, mixing images from different classes versus using class-homogeneous batches, and prompting with either class names or class IDs are assessed. The outcomes are provided in the Supplementary. The best-performing parameters are selected and used throughout all the experiments.

3.1. Closed-World

Results on original labels. The results of all models are reported in the first column of Tab. 4. Among the MLLMs, PaliGemma 2 scores 37%, while LLaVA-OV (62%) and InternVL3.5 (64%) are close to Qwen3-VL (69%), which is in turn outperformed by GPT-4o (76%). Despite this impressive result, there is still a gap between

GPT-4o and vision-specific self-supervised models, with the leading VLM SigLIP 2 ViT/g-opt-384 reaching 84%. The supervised models still outperform all others, with EfficientNetV2-XL and EfficientNet-L2 scoring 85% and 88%, respectively, while EVA-02 achieves the highest accuracy of 90%.

Results on reannotated labels. Across all MLLMs, reannotation yields the largest gains of any model family: PaliGemma 2 improves by 10.8%, LLaVA-OV by 8.6%, InternVL3.5 by 8.3%, Qwen3-VL by 7.9%, and GPT-4o by 6.0%. The performance of VLMs still shows a solid improvement of 3–4.1%. Supervised models improve less. EfficientNetV2-XL gains 1.3% on the reannotated labels, while EfficientNet-L2 improves by 0.7% and EVA-02 slightly decreases by 0.1%. This confirms the intuition that the more a model relies on the training data, the smaller the benefit from reannotation. The results also show VLMs and MLLMs are not overfitted to the official ImageNet-1k validation labels, as reflected on the S- and M- subsets, where the top ranks go to self-supervised models rather than supervised ones. Deltas between ImGT and ReGT are presented in Fig. 3.

Notably, the gap between MLLMs and supervised models got reduced significantly, for the better performing GPT-4o by roughly 6%. As shown in Tab. 2, our non-OOD reannotated labels do not contain the ground-truth label in 9.6% of images (S-, M-), which is close to the error rate of the best-performing supervised model EVA-02.

Out-Of-Prompt. MLLMs still often predict texts outside of the provided prompt class names despite clear instructions not to, an effect often referred to as hallucinations [21, 45]. We investigate this in Tab. 5 based on the label categories.

NN in text embedding space mapping (CW+). To address the OOP issue discussed earlier, we encode the predic-

		ImGT			ReGT				
Task		A ₃₁₂₅₀	A ₃₁₂₅₀	S ₁₈₀₇₁	S ₊₁₆₁₇₇	S ₋₁₈₉₄	M ₁₁₈₃₄	M ₊₁₀₇₅₆	M ₋₁₀₇₈
PaliGemma 2	OW	37.11	47.94	39.74	41.49	24.76	54.55	56.24	37.66
LLaVA-OV	OW	62.00 +18.6	70.58 +17.8	67.11 +17.5	70.67 +18.7	36.69 +7.1	72.52 +20.3	75.87 +22.0	39.05 +4.1
	CW+	52.66 +9.3	62.82 +10.1	59.54 +10.0	62.32 +10.4	35.80 +6.2	63.61 +11.4	65.84 +11.9	41.37 +6.4
	CW	43.40	52.75	49.59	51.94	29.57	52.20	53.92	34.97
InternVL3.5	OW	59.23 -4.9	68.18 -4.2	62.44 -5.1	65.78 -5.1	33.90 -5.1	73.33 -3.5	76.66 -3.7	40.07 -1.4
	CW+	64.31 +0.2	72.57 +0.2	67.69 +0.2	71.05 +0.2	39.02 +0.0	76.91 +0.1	80.43 +0.1	41.74 +0.3
	CW	64.14	72.42	67.51	70.84	39.02	76.78	80.32	41.47
Qwen3-VL	OW	68.74 +4.9	76.68 +5.3	73.61 +3.5	77.79 +3.7	37.91 +1.9	78.71 +8.7	82.46 +8.9	41.28 +7.0
	CW+	66.74 +2.9	74.43 +3.0	72.90 +2.8	76.95 +2.8	38.23 +2.2	73.86 +3.8	77.53 +3.9	37.29 +3.0
	CW	63.86	71.39	70.15	74.14	36.06	70.04	73.61	34.32
GPT-4o	OW	70.92 -4.5	77.58 -3.7	76.59 -3.7	81.08 -4.3	38.23 +1.2	76.55 -4.1	80.75 -4.4	34.69 -1.6
	CW+	76.40 +1.0	82.36 +1.1	81.11 +0.8	86.12 +0.7	38.28 +1.2	82.27 +1.6	86.74 +1.6	37.66 +1.4
	CW	75.40	81.29	80.32	85.39	37.06	80.65	85.10	36.27

Table 6. Recognition accuracy for CW(+) and OW tasks. PaliGemma 2 results are reported only for the OW setup, since it is not feasible to perform CW with all class names included in a single prompt. Changes relative to the Closed World (CW) baseline are indicated as **increases** or **decreases**. The CW+ setup extends the CW task by applying the same text-embedding-space output mapping used in the Open World (OW) task, addressing OOP predictions in CW that would otherwise be considered incorrect. Results are obtained using the best-performing model-specific encoder; for a comparison of all encoders, see Tab. 18. As expected, accuracy in CW+ is higher than in standard CW. Notably, LLaVA-OV and Qwen3-VL outperform their CW results in the OW setup, an unexpected trend that contrasts prior findings on MLLMs [21, 45]. In contrast, InternVL3.5 and GPT-4o achieve the highest performance in CW+.

		ImGT			ReGT				
Distractors		A ₆₂₅	A ₆₂₅	S ₃₅₂	S ₊₃₁₆	S ₋₃₆	M ₂₄₀	M ₊₂₂₁	M ₋₁₉
GPT-4o	ImGT + random	99.62 ±0.07	90.95 ±0.05	89.49 ±0.07	99.67 ±0.07	0.09 ±0.18	91.85 ±0.10	99.75 ±0.11	0.00 ±0.00
	ImGT + confEVA (ImGT)	90.66 ±0.22	85.12 ±0.21	84.27 ±0.26	93.87 ±0.29	0.00 ±0.00	84.31 ±0.39	91.56 ±0.42	0.00 ±0.00
	ReGT + confEVA (ReGT)	51.35 ±0.21	84.26 ±0.37	92.45 ±0.36	93.90 ±0.31	79.66 ±1.50	70.09 ±0.89	70.78 ±0.83	62.14 ±3.36
	ImGT + ReGT + random	91.77 ±0.26	94.89 ±0.13	94.79 ±0.16	99.67 ±0.07	51.97 ±1.35	94.31 ±0.27	99.80 ±0.09	30.56 ±2.97
	ImGT + ReGT + confEVA (ImGT, ReGT)	88.31 ±0.29	92.52 ±0.15	91.59 ±0.20	96.36 ±0.15	49.73 ±1.27	92.86 ±0.31	98.16 ±0.20	31.24 ±3.30
	ImGT + 999 (Closed World (CW))	74.69 ±0.19	81.32 ±0.18	79.87 ±0.19	84.49 ±0.21	39.25 ±0.82	80.89 ±0.35	84.72 ±0.36	36.33 ±0.58

Table 7. 4-way multiple-choice (MC) task results on a randomly sampled subset of 625 images (one per class) with 95 % confidence intervals (CI). The function `confEVA()` generates challenging distractors based on the confusion matrix of EVA-02. The Closed World result corresponds to 999 distractors. Only GPT-4o results are shown here, as the trend of gradually declining accuracy with more challenging distractors is similar across models. Full multiple-choice task results for all evaluated MLLMs are provided in Tab. 19.

tions from models into the text embedding space (similarly to the OW setup), so that the predicted outputs are semantically aligned with the provided class names. Each predicted text embedding is then assigned to its nearest class name embedding. The results, denoted as CW+, are shown in Tab. 6. The performance of CW+ consistently outperforms pure CW across all subsets and models, with the most pronounced improvements observed on the more challenging S- and M- subsets. We observe that the overall accuracy improvement achieved by LLaVA-OV (the highest among all evaluated models) is approximately 54× greater than that of InternVL3.5 (the model with the lowest improvement) when evaluated against the original ImageNet-1k ground-truth labels, and approximately 67× greater when evaluated

using the reannotated labels. This pronounced difference can be attributed to the substantially higher OOP rate exhibited by LLaVA-OV across all label categories (Tab. 5). Notably, the correct mapping rate scales with the overall OOP rate. A comprehensive breakdown of mapping results across all models and categories is provided in the supplementary (see Tab. 15). Representative examples of successful mappings are shown in Fig. 4.

3.2. Multiple-Choice

The results in Tab. 7 reveal the commonly adopted setup with random distractors significantly inflates the performance. Providing more challenging distractors makes the performance drop by 10-15 %. The results also show that if



Figure 5. Images from the second annotation pass, where annotators 1. preferred GPT-4o prediction over the reannotated labels (left), 2. retained at least part of the reannotated labels without adding GPT-4o prediction (right), and 3. combined reannotations with GPT-4o predictions (middle). “ImGT” stands for ImageNet-1k ground truth, “ChatGPT” denotes GPT-4o prediction for the image, “ReGT” refers to first pass reannotations, and “ReReGT” indicates second pass reannotations. Annotators in the second pass not only preserved correct ReGT or added GPT-4o predictions, but also identified and corrected erroneous labels from the first pass.

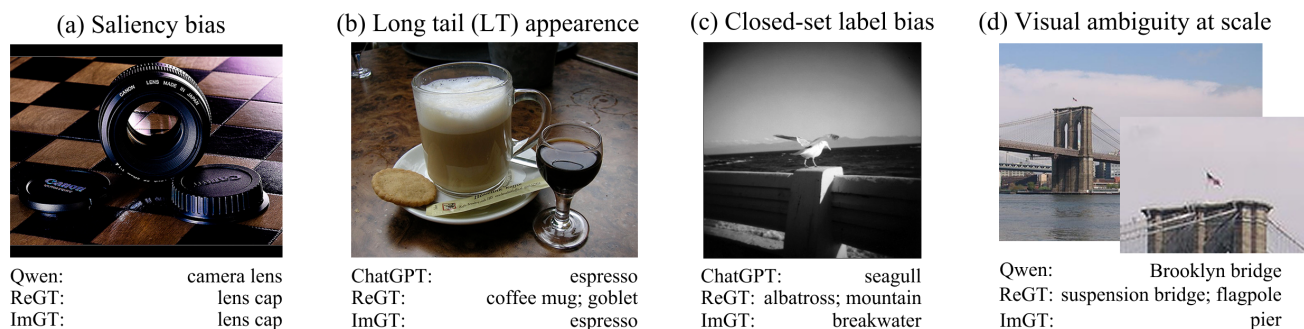


Figure 6. Challenging classification cases. (a): The dominant object, which MLLMs tend to predict, does not always correspond to the intended class. Here, the dominant object, the lens, \notin ImageNet-1k class list. (b): Appearance variations make it difficult to recognize long-tail content without additional context. An espresso served in a goblet for latte preparation differs from the typical presentation in a cup, confusing models and humans alike. (c): Fixed class lists push annotators/models to select a label, even when the image content falls outside the defined categories (“seagull” \notin ImageNet-1k). (d): Recognizability depends on scale and perceptual context. For smaller or visually ambiguous objects, determining what is seen versus inferred by contextual associations becomes increasingly challenging.

we provide the models with both original and reannotated GT, both models seem to choose between them at an equal rate on challenging single label images where the reannotated label differs (S−). Finally, it can be observed the confidence intervals are wider on the challenging S− and M−.

3.3. Open-World

The MLLMs performance in the free-form output setup is reported in Tab. 6. The results indicate that overall perfor-

mance is noticeably lower than in the CW setup for InternVL3.5 ($\approx 5\%$) and GPT-4o ($\approx 4\%$), whereas it is higher than the CW setup for LLaVA-OV ($\approx 19\%$) and Qwen3-VL ($\approx 5\%$). This latter observation contrasts with previous studies [21, 45], which reported that accuracy in the CW setup generally exceeds that of the OW setup for various MLLMs - a trend we also observe for InternVL3.5 and GPT-4o. In the OW setup, Qwen3-VL even surpasses GPT-4o’s performance in both CW and OW on M−. Con-

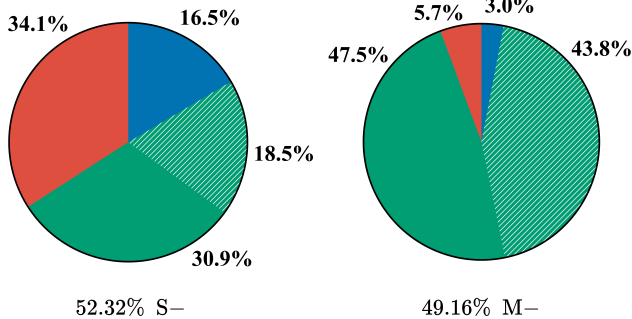


Figure 7. Second annotation pass results on images where GPT-4o gave a valid prediction and disagreed with ReGT labels for S- and M- label categories (which are challenging, since $\text{ImGT} \notin \text{ReGT}$). Color coding: Annotators \blacksquare preferred in the second, verification pass, the GPT-4o prediction (ReGT was incorrect); \blacksquare preserved reannotated labels without adding GPT-4o prediction (ReGT was correct); ▨ combined GPT-4o prediction with reannotated labels (GPT-4o \notin ReGT before); \blacksquare made other changes (GPT-4o prediction and ReGT \notin new labels). The percentage values below the pie charts represent the proportions of S- and M- images for which the valid GPT-4o prediction is obtained, differing from the ReGT.

sistent with the CW results, all models show substantial improvement on the reannotated labels compared to the original labels.

3.4. Case study: ChatGPT vs. humans

We conducted a second annotation pass by randomly assigning all challenging S- (1894) and M- (1078) images to our annotators. For each image, annotators received the following in random, anonymized order: 1. GPT-4o prediction, 2. ReGT, 3. ImGT, and 4. SigLIP 2 giant prediction. GPT-4o was prompted to return all ImageNet-1k labels present in an image as class IDs rather than full class names, reducing token usage and associated costs.

ChatGPT accuracy on S- and M- images was initially 34.37% and 34.32%, respectively, with respect to ReGT. After the second pass, accuracy increased to 55.20% and 55.19%. An analysis of the results from this verification pass is presented in Fig. 7. For 52.6% of S- and 49.5% of M- images ($\blacksquare + \text{▨}$ sections in Fig. 7), annotators either confirmed the ChatGPT prediction as the only correct label or combined it with the ReGT label.

There remains a set of 30.9% S- and 47.5% M- mispredicted images (\blacksquare sections in Fig. 7) where at least some of the ReGT labels were preserved and no ChatGPT predictions were added. Examples of these reannotations are presented in Fig. 5. We conclude: 1. Error corrections made by trained annotators are not entirely reliable, being completely incorrect ($\blacksquare + \blacksquare$) in 50.6% of S- and 8.7% of M- images; and 2. ChatGPT can serve as a valuable assistant for flagging such errors for additional verification.

4. Conclusions

We presented an evaluation of both closed- and open-source MLLMs on ImageNet-1k, enabled by a new large-scale re-annotation that substantially reduces label noise and clarifies long-standing ambiguities. The analysis shows that MLLMs perceived performance is most affected by incorrect ground truth. GT corrections narrowed the apparent performance gap w.r.t. supervised and self-supervised vision models, while also revealing strong MLLMs sensitivity to task formulation and distractor selection. The re-annotated labels further expose how model families differ in their robustness to mislabeled and multilabel images, and demonstrate that MLLMs can meaningfully assist human annotators in a controlled curation pipeline. Although closed-source systems retain an advantage under strict Closed-World prompting, this gap largely disappears in Open-World settings.

In Fig. 6, we highlight some challenges of image classification and annotation. Overall, our findings show both the promise and the current limitations of MLLMs for visual recognition, underscoring the need for cleaner benchmarks, principled evaluation protocols, and careful integration of model assistance in dataset construction.

References

- [1] Anthropic. Claude 3, 2025. [Large language model]. 1
- [2] Jinze Bai, Shuai Bai, Shusheng Yang, Shijie Wang, Sinan Tan, Peng Wang, Junyang Lin, Chang Zhou, and Jingren Zhou. Qwen-vl: A versatile vision-language model for understanding, localization, text reading, and beyond, 2023. 1
- [3] Lucas Beyer, Olivier J. Hénaff, Alexander Kolesnikov, Xiaoohua Zhai, and Aaron van den Oord. Are we done with imagenet?, 2020. 2, 3, 4
- [4] Tom B. Brown, Benjamin Mann, Nick Ryder, Melanie Subbiah, and Jared Kaplan et. al. Language models are few-shot learners, 2020. 1
- [5] Davide Caffagni, Federico Cocchi, Luca Barsellotti, Nicholas Moratelli, Sara Sarto, Lorenzo Baraldi, Lorenzo Baraldi, Marcella Cornia, and Rita Cucchiara. The revolution of multimodal large language models: A survey, 2024. 1
- [6] Zhe Chen, Jiannan Wu, Wenhai Wang, Weijie Su, Guo Chen, Sen Xing, Muyan Zhong, Qinglong Zhang, Xizhou Zhu, Lewei Lu, Bin Li, Ping Luo, Tong Lu, Yu Qiao, and Jifeng Dai. Internvl: Scaling up vision foundation models and aligning for generic visual-linguistic tasks, 2024. 1, 2, 4
- [7] Alessandro Conti, Massimiliano Mancini, Enrico Fini, Yiming Wang, Paolo Rota, and Elisa Ricci. On large multimodal models as open-world image classifiers, 2025. 2, 12, 16, 22
- [8] Google DeepMind. Gemini, 2025. [Large language model]. 1
- [9] Matt Deitke, Christopher Clark, Sangho Lee, Rohun Tripathi, Yue Yang, and Jae Sung Park et al. Molmo and pixmo: Open weights and open data for state-of-the-art vision-language models, 2024. 1

- [10] Jacob Devlin, Ming-Wei Chang, Kenton Lee, and Kristina Toutanova. BERT: Pre-training of deep bidirectional transformers for language understanding. In *Proceedings of the 2019 Conference of the North American Chapter of the Association for Computational Linguistics: Human Language Technologies, Volume 1 (Long and Short Papers)*, pages 4171–4186, Minneapolis, Minnesota, 2019. Association for Computational Linguistics. 12
- [11] Jacob Devlin, Ming-Wei Chang, Kenton Lee, and Kristina Toutanova. Bert: Pre-training of deep bidirectional transformers for language understanding, 2019. 1
- [12] Yuze Du, Yingjia Wang, and Eric Zhao. Leveraging multimodal llms for plant species identification and educational insights, 2024. 1
- [13] Chaoyou Fu, Peixian Chen, Yunhang Shen, Yulei Qin, Mengdan Zhang, Xu Lin, and Jinrui Yang et al. Mme: A comprehensive evaluation benchmark for multimodal large language models, 2025. 1, 4, 12
- [14] Manu Gaur, Darshan Singh S, and Makarand Tapaswi. Detect, describe, discriminate: Moving beyond vqa for mllm evaluation, 2024. 12
- [15] Hongliang He, Wenlin Yao, Kaixin Ma, Wenhao Yu, Yong Dai, Hongming Zhang, Zhenzhong Lan, and Dong Yu. Webvoyager: Building an end-to-end web agent with large multimodal models, 2024. 1
- [16] Nikita Kisel, Illia Volkov, Kateřina Hanzelková, Klara Janouskova, and Jiri Matas. Flaws of imagenet, computer vision’s favourite dataset. In *The Fourth Blogpost Track at ICLR 2025*, 2025. 2, 3, 4, 6, 12, 13, 14
- [17] Bohao Li, Rui Wang, Guangzhi Wang, Yuying Ge, Yixiao Ge, and Ying Shan. Seed-bench: Benchmarking multimodal llms with generative comprehension, 2023. 1, 4, 12
- [18] Bo Li, Yuanhan Zhang, Dong Guo, Renrui Zhang, Feng Li, Hao Zhang, Kaichen Zhang, Peiyuan Zhang, Yanwei Li, Ziwei Liu, and Chunyuan Li. Llava-onevision: Easy visual task transfer, 2024. 2, 4
- [19] Chunyuan Li, Cliff Wong, Sheng Zhang, Naoto Usuyama, Haotian Liu, Jianwei Yang, Tristan Naumann, Hoifung Poon, and Jianfeng Gao. Llava-med: Training a large language-and-vision assistant for biomedicine in one day, 2023. 1
- [20] Haotian Liu, Chunyuan Li, Qingyang Wu, and Yong Jae Lee. Visual instruction tuning, 2023. 1
- [21] Huan Liu, Lingyu Xiao, Jiangjiang Liu, Xiaofan Li, Ze Feng, Sen Yang, and Jingdong Wang. Revisiting mllms: An in-depth analysis of image classification abilities, 2024. 1, 2, 6, 7, 8, 12, 16
- [22] Haowei Liu, Xi Zhang, Haiyang Xu, Yaya Shi, Chaoya Jiang, Ming Yan, and Ji Zhang et al. Mibench: Evaluating multimodal large language models over multiple images, 2024. 1, 4, 12
- [23] Yuan Liu, Haodong Duan, Yuanhan Zhang, Bo Li, Songyang Zhang, and Wangbo Zhao et al. Mmbench: Is your multimodal model an all-around player?, 2024. 1, 4, 12
- [24] Alexandra Sasha Luccioni and David Rolnick. Bugs in the data: How imagenet misrepresents biodiversity, 2022. 3
- [25] Curtis G. Northcutt, Anish Athalye, and Jonas Mueller. Pervasive label errors in test sets destabilize machine learning benchmarks, 2021. 2, 3
- [26] OpenAI. Chatgpt (gpt-5), 2025. [Large language model]. 1
- [27] OpenAI et al. Gpt-4o system card, 2024. 1, 2, 4
- [28] Alec Radford, Jeff Wu, Rewon Child, David Luan, Dario Amodei, and Ilya Sutskever. Language models are unsupervised multitask learners. 2019. 1
- [29] Alec Radford, Jong Wook Kim, Chris Hallacy, Aditya Ramesh, Gabriel Goh, Sandhini Agarwal, Girish Sastry, Amanda Askell, Pamela Mishkin, Jack Clark, Gretchen Krueger, and Ilya Sutskever. Learning transferable visual models from natural language supervision, 2021. 1, 6, 22
- [30] Colin Raffel, Noam Shazeer, Adam Roberts, Katherine Lee, Sharan Narang, Michael Matena, Yanqi Zhou, Wei Li, and Peter J. Liu. Exploring the limits of transfer learning with a unified text-to-text transformer, 2023. 1
- [31] Nils Reimers and Iryna Gurevych. Sentence-bert: Sentence embeddings using siamese bert-networks, 2019. 12, 16
- [32] Vaishaal Shankar, Rebecca Roelofs, Horia Mania, Alex Fang, Benjamin Recht, and Ludwig Schmidt. Evaluating machine accuracy on ImageNet. In *Proceedings of the 37th International Conference on Machine Learning*, pages 8634–8644. PMLR, 2020. 2
- [33] Andreas Steiner, André Susano Pinto, Michael Tschannen, Daniel Keysers, Xiao Wang, Yonatan Bitton, Alexey Gritsenko, Matthias Minderer, Anthony Sherbondy, Shangbang Long, Siyang Qin, Reeve Ingle, Emanuele Bugliarello, Sahar Kazemzadeh, Thomas Mesnard, Ibrahim Alabdulmohsin, Lucas Beyer, and Xiaohua Zhai. Paligemma 2: A family of versatile vlms for transfer, 2024. 2, 4
- [34] Mingxing Tan and Quoc V. Le. Efficientnetv2: Smaller models and faster training, 2021. 5
- [35] Michael Tschannen, Alexey Gritsenko, Xiao Wang, Muhammad Ferjad Naeem, Ibrahim Alabdulmohsin, Nikhil Parthasarathy, Talfan Evans, Lucas Beyer, Ye Xia, Basil Mustafa, Olivier Hénaff, Jeremiah Harmsen, Andreas Steiner, and Xiaohua Zhai. Siglip 2: Multilingual vision-language encoders with improved semantic understanding, localization, and dense features, 2025. 1, 5, 16
- [36] Dimitris Tsipras, Shibani Santurkar, Logan Engstrom, Andrew Ilyas, and Aleksander Madry. From imagenet to image classification: Contextualizing progress on benchmarks, 2020. 2, 3
- [37] Tao Tu, Shekoofeh Azizi, Danny Driess, and Mike Schaekermann et al. Towards generalist biomedical ai, 2023. 1
- [38] Vijay Vasudevan, Benjamin Caine, Raphael Gontijo-Lopes, Sara Fridovich-Keil, and Rebecca Roelofs. When does dough become a bagel? analyzing the remaining mistakes on imagenet, 2022. 2, 4
- [39] Ross Wightman. Pytorch image models. <https://github.com/rwightman/pytorch-image-models>, 2019. 5
- [40] Wenhao Wu, Huanjin Yao, Mengxi Zhang, Yuxin Song, Wanli Ouyang, and Jingdong Wang. Gpt4vis: What can gpt-4 do for zero-shot visual recognition?, 2024. 1, 2
- [41] An Yang, Anfeng Li, Baosong Yang, Beichen Zhang, Binyuan Hui, Bo Zheng, Bowen Yu, Chang Gao, Chengen Huang, Chenxu Lv, and Chujie Zheng et al. Qwen3 technical report, 2025. 2, 4, 16

- [42] Shukang Yin, Chaoyou Fu, Sirui Zhao, Ke Li, Xing Sun, Tong Xu, and Enhong Chen. A survey on multimodal large language models. *National Science Review*, 11(12), 2024. [1](#)
- [43] Sangdoon Yun, Seong Joon Oh, Byeongho Heo, Dongyoon Han, Junsuk Choe, and Sanghyuk Chun. Re-labeling imagenet: from single to multi-labels, from global to localized labels, 2021. [2](#), [3](#)
- [44] Xiaohua Zhai, Basil Mustafa, Alexander Kolesnikov, and Lucas Beyer. Sigmoid loss for language image pre-training, 2023. [1](#), [4](#)
- [45] Yuhui Zhang, Alyssa Unell, Xiaohan Wang, Dhruva Ghosh, Yuchang Su, Ludwig Schmidt, and Serena Yeung-Levy. Why are visually-grounded language models bad at image classification?, 2024. [1](#), [2](#), [6](#), [7](#), [8](#), [12](#)
- [46] Kaiyang Zhou, Jingkang Yang, Chen Change Loy, and Ziwei Liu. Learning to prompt for vision-language models. *International Journal of Computer Vision*, 130(9):2337–2348, 2022. [6](#)
- [47] Kaiyang Zhou, Jingkang Yang, Chen Change Loy, and Ziwei Liu. Conditional prompt learning for vision-language models, 2022. [6](#)

Multimodal Large Language Models as Image Classifiers

Supplementary Material

A. Related Work

MLLM evaluation. MLLMs benchmarks [13, 17, 22, 23] have largely converged on multiple-choice question answering as the dominant evaluation format, favored for its simplicity and unambiguous scoring. However, this format makes direct comparison with traditional vision models (VLMs, supervised classifiers) difficult, as it measures different capabilities. Some benchmarks [17, 22] design more challenging distractors, while others [14] argue that selecting from a list is fundamentally easier than generating an answer, promoting self-retrieval methods that test a model’s ability to describe and distinguish images without provided options. Our work fills this gap by evaluating MLLMs on standard image classification under conditions comparable to traditional vision models.

MLLMs in Image Classification. Zhang et al. [45] show that generative MLLMs perform far below CLIP on ImageNet-1k, even in a Closed-World task, though limited to 100 classes due to token length constraints of older models. To address OOP predictions, they introduce Probabilistic Inference, which constrains generation to only tokens from the provided class list. While effective, this is computationally intensive: for 1,000 classes, inference is 1,000 times slower than direct generation. This contrasts with our CW+ approach, which resolves OOP via fast post-processing. The authors also evaluate an OW task, using string matching (*i.e.* text inclusion) to map free-text predictions to class names. This mapping strategy is inefficient, which explains why they find OW to always perform worse than CW — a finding we do not replicate with our embedding-based mapping.

Liu et al. [21] report that newer MLLMs approach or surpass CLIP-like systems, though typically under MC conditions. They explore increasing the number of answer options up to 26 — the number of letters in the alphabet — and find that accuracy decreases as options grow. To increase difficulty, they construct harder distractors using the top-25 most semantically similar class names identified with BERT [10], observing only a slight accuracy drop of 2.3 percentage points for Qwen2-VL on ImageNet-1k. Notably, their experiments are run once without confidence intervals. Our confidence-interval-backed experiments show a considerably larger accuracy drop under their sampling strategy, and a further increase with our harder distractor selection strategy. Similarly to [45], the authors do not evaluate on the full class list due to OOP, a limitation we address with CW+.

Conti et al. [7] evaluate MLLMs in an Open-World task

across several metrics, including cosine similarity between model predictions and ground-truth labels in the Sentence-BERT [31] embedding space, which is an inspiration for our embedding-space approach, but we utilize newer models. We additionally include experiments with their encoder in Tab. 18. However, they do not report results for ImageNet-1k and focus solely on MLLMs and the OW task, whereas we also observe performance on other tasks, and compare it against VLMs and supervised models.

B. Evaluation Setup - Details

B.1. Prompt overview

The exact prompts used for InternVL3.5, LLaVA-OV, Qwen3-VL, and GPT-4o are provided in Tab. 20 for the CW and CW+ tasks, and in Tab. 21 for the OW task. In the MC setup, all models share the same prompt, as shown in Tab. 22, whereas the OW and CW prompts differ. A key distinction is that GPT-4o prompts generally omit detailed instructions on output formatting, since the desired output structure is enforced directly via the API. For PaliGemma 2, the standard `describe en` prompt was employed in the OW setup. The CW task could not be performed due to the input prompt exceeding the token length limit.

B.2. Classification task decomposition

We provide a detailed breakdown of task components in Tab. 8, including the input prompt format and the output processing. A “Notes” column is also included to highlight the subtleties defined by each task.

B.3. Equal classes

We list all class pairs treated as equal for evaluation in the main paper, along with image examples and brief explanations, in Fig. 10 and Fig. 11.

B.4. Weasel family case study

The reannotated dataset, as introduced in Sec. 2.1, only contains 625 out of the original 1000 classes, where the majority of wildlife, with the prominent exception of about 120 dog breeds, is excluded.

This is because wildlife is notoriously hard to annotate for non-experts, even if the annotators are trained. To account for this limitation, we also introduce a case study on four classes from the weasel family: weasel, mink, polecat and black-footed ferret, whose reannotation conducted by an expert was introduced in [16]. For a brief overview of the classes and image examples, see Fig. 8.

Task	Prompt Format	Output Processing	Notes
OW	Few-shot text examples included	LM embedding-space matching	Depends on embedding alignment
CW	All class names listed	Exact string matching	Simple but requires full class list
CW+	All class names listed	LM embedding-space matching	Embedding-based encoding adds complexity
MC	Image-specific question with labeled options	Letter matching	Must map image-specific options correctly; performance highly depends on distractor choices

Table 8. Decomposition of evaluated MLLMs image classification tasks. LM stands for language model. The “Notes” column highlights the main complication or subtlety in each task setup.



Figure 8. Weasel family case study: Class overview. Correctly labeled ImageNet-1k images from the “weasel”, “mink”, “polecat”, and “black-footed ferret” classes are shown. (a) The term ‘**weasel**’ is often used to describe the whole *mustelidae* family, which encompasses all the four species, but the images correspond to the least weasel species and similar. (b) **Minks** are easier to recognize, but still easily confused with the others for non-experts. (c) The European **polecat** is the ancestor of domestic ferret and they are extremely hard to recognize and they can also interbreed. Often, they are recognized by the environment (domestic ferrets are typically found in a man-made environment, polecats in the wild), as opposed by the animals’ features. For this reason, the images are a mix. (d) The **black-footed ferret** is a rare ferret species and most images are actually the domesticated ferret, easily confused with polecats, as explained previously. The class got renamed to ‘domestic ferret’. For more details on the reannotation and the issues, please refer to Kisel et. al. [16].

The weasel problem. Here we provide a brief overview of the classes and the main issues. For more details, we refer the reader to the original publication.

Kisel et al. [16] revisited four closely related mustelid classes in ImageNet and found severe problems arising from ambiguous synsets, inconsistent taxonomy, and extensive mislabeling. Their expert reannotation shows that these fine-grained wildlife categories cannot reliably serve as ground truth. The main issues are:

- **weasel:** Synset corresponds to a broad colloquial category rather than a specific species; many images depict other mustelids (e.g., mink, ferrets), leading to more than half of the images being incorrect. However, the dominant species is the least weasel and highly similar species. In American English, the term weasel often refers to the weasel family as a whole, encompassing all four classes.
- **mink:** Although somewhat cleaner, many images still mix American and European mink and include other small mustelids due to visual similarity and poor source metadata.
- **polecat (*Mustela putorius*):** The term “polecat” is ambiguous across English varieties and is also used for skunks; images contain a heterogeneous mix of species, and only about one-third match the intended European polecat. The European polecat is the ancestor of the domestic ferret, which makes them hard to distinguish, and

they can also interbreed.

- **black-footed ferret (*Mustela nigripes*):** Synset conflates the endangered wild species with domestic ferrets; almost all images show domestic animals rather than *M. nigripes*, leaving the class effectively without valid examples. The class is renamed to ‘domestic ferret’.

These issues stem from WordNet synset definitions that do not align with real-world photographic data, making the original ImageNet labels highly unreliable for fine-grained species evaluation.

Performance on reannotated data. Across model families, accuracy generally increases when evaluated on the reannotated labels, with substantially larger gains on the 159-image WeaselGT subset, see Tab. 9. The improvements are most pronounced for MLLMs and VLMs, indicating that many of their apparent errors under the original ImGT labels stem from annotation noise. In contrast, supervised models show smaller gains, suggesting stronger anchoring to the original label space. Tab. 10 complements this by reporting class-level recall under the original ImGT labels versus WeaselGT labels. Taken together, the tables show that careful reannotation is essential for reliably evaluating model performance on closely related wildlife categories.

Model	Task	ImGT		ReGT	WeaselGT		
		A ₆₂₅	A ₁₅₉ 🐾	A ₆₂₅	A ₁₅₉ 🐾	S ₊₁₁₂	S ₋₄₇
ImGT	CW	100.00	100.00	91.20 -8.8	70.44 -29.6	100.00	00.00
LLaVA-OV	CW	42.56	25.79	52.00 +9.4	28.93 +3.1	35.71	12.77
	MC	82.17	45.91	90.01 +7.8	61.01 +15.1	59.82	63.83
Intern-VL3.5	CW	63.68	44.65	72.96 +9.3	61.01 +16.4	60.71	61.70
	MC	85.89	55.97	90.53 +4.6	75.47 +19.5	75.89	74.47
Qwen3-VL	CW	64.16	40.25	72.16 +8.0	50.94 +10.7	54.46	42.55
	MC	86.32	64.15	90.77 +4.5	83.65 +19.5	86.61	76.60
GPT-4o	CW	74.69	64.15	81.32 +6.6	84.28 +20.1	88.39	74.47
	MC	88.31	67.92	92.52 +4.2	91.19 +23.3	92.86	87.23
DINOv3 (dino.txt)	CW	79.36	69.18	85.12 +5.8	86.79 +17.6	91.96	74.47
SigLIP so400M	CW	82.88	66.04	87.20 +4.3	88.05 +22.0	91.07	80.85
SigLIP 2 so400M	CW	83.36	66.67	87.68 +4.3	88.68 +22.0	90.18	85.11
SigLIP 2 giant	CW	83.84	67.92	86.24 +2.4	91.82 +23.9	92.86	89.36
DINOv3 (<i>k</i> -NN)	CW	83.36	71.07	87.20 +3.8	79.87 +8.8	87.50	61.70
EfficientNetV2-XL	CW	85.12	71.07	86.88 +1.8	78.62 +7.6	87.50	57.45
EfficientNet-L2	CW	87.52	75.47	89.12 +1.6	80.50 +5.0	91.07	55.32
EVA-02	CW	90.24	73.58	91.68 +1.4	80.50 +6.9	90.18	57.45

Table 9. Weasel family case study results. Accuracy on the reannotated weasel-family subset for ImGT and MLLMs (top), VLMs (center) and supervised models (bottom). Columns report accuracy on the full 31,250-image reannotated set and on the WeaselGT 159-image subset 🐾. Increase or decrease indicates the change in accuracy when evaluating on ReGT labels instead of the original ImGT labels. For WeaselGT, deltas denote the difference between WeaselGT labels and the original ImGT labels on the same 159-image subset 🐾. Overall, the consistently positive gains on WeaselGT largest for VLMs and MLLMs and comparatively modest for supervised models suggest that multimodal and vision-language models are more sensitive to finegrained semantic corrections introduced by the reannotations, whereas supervised models remain more anchored to the original label space.

	weasel		mink		polecat		domestic ferret	
	ImGT	WeaselGT	ImGT	WeaselGT	ImGT	WeaselGT	ImGT	WeaselGT
ImGT	100.00	84.62 -15.4	100.00	85.00 -15.0	100.00	57.14 -42.9	100.00	61.54 -38.5
LLaVA-OV	40.00	76.92 +36.9	60.00	65.00 +5.0	0.00	0.00 +0.0	0.00	0.00 +0.0
Intern-VL3.5	30.00	65.38 +35.4	32.00	37.50 +5.5	0.00	0.00 +0.0	92.00	100.00 +8.0
Qwen3-VL	36.00	76.92 +40.9	72.00	80.00 +8.0	0.00	3.57 +3.6	42.00	43.08 +1.1
GPT-4o	46.00	100.00 +54.0	94.00	95.00 +1.0	10.00	17.86 +7.9	92.00	100.00 +8.0
DINOv3 (dino.txt)	44.00	92.31 +48.3	92.00	100.00 +8.0	36.00	64.29 +28.3	84.00	86.15 +2.2
SigLIP so400M	42.00	88.46 +46.5	94.00	97.50 +3.5	26.00	57.14 +31.1	86.00	95.38 +9.4
SigLIP 2 so400M	44.00	92.31 +48.3	92.00	95.00 +3.0	30.00	67.86 +37.9	86.00	92.31 +6.3
SigLIP 2 giant	44.00	100.00 +56.0	94.00	97.50 +3.5	34.00	78.57 +44.6	78.00	90.77 +12.8
DINOv3 (<i>k</i> -NN)	48.00	100.00 +52.0	94.00	100.00 +6.0	48.00	71.43 +23.4	74.00	63.08 -10.9
EfficientNetV2-XL	48.00	96.15 +48.2	92.00	100.00 +8.0	60.00	85.71 +25.7	62.00	55.38 -6.6
EfficientNet-L2	52.00	100.00 +48.0	96.00	100.00 +4.0	66.00	82.14 +16.1	74.00	60.00 -14.0
EVA-02	52.00	100.00 +48.0	96.00	100.00 +4.0	60.00	82.14 +22.1	74.00	60.00 -14.0

Table 10. Recall on the original ImGT labels compared to the WeaselGT labels. For ImGT, we evaluate on 50 images per class based on the original annotations; for WeaselGT, we use the class assignments provided in [16]. MLLMs (top) show substantial recall increases under WeaselGT, often reaching perfect recall, indicating that many of their apparent “errors” under ImGT stem from mislabeled or ambiguous images. Note: for MLLMs, the recall is computed only for the CW setup. VLMs (center) also improve, suggesting lingering sensitivity to finegrained distinctions. Supervised models (bottom) sometimes exhibit substantial drops in recall on WeaselGT, suggesting that they overfit to the ImGT. Overall, the shift from ImGT to WeaselGT indicates that MLLMs and VLMs are more robust to annotation noise.

	Batch	ImGT			ReGT					
		A ₆₂₅	A ₆₂₅	S ₃₅₂	S ₊₃₁₆	S ₋₃₆	M ₂₄₀	M ₊₂₂₁	M ₋₁₉	OOP
LLaVA-OV	1	42.56	52.00	46.31	48.10	30.56	53.75	55.20	36.84	168
	5	34.88	42.56	37.78	40.19	16.67	41.67	43.44	21.05	233
	10	27.20	35.36	30.97	32.28	19.44	32.92	34.39	15.79	258
Qwen3-VL	1	64.96	73.12	69.32	73.10	36.11	75.00	77.83	42.11	28
	5	63.52	72.00	70.45	74.37	36.11	70.42	72.85	42.11	44
	10	64.16	72.16	71.88	75.95	36.11	68.75	72.40	26.32	61
GPT-4o	1	73.92	80.80	79.55	84.49	36.11	80.00	83.71	36.84	23
	5	74.40	81.76	80.40	84.81	41.67	81.25	85.07	36.84	27
	10	74.24	81.92	80.68	85.44	38.89	81.25	85.07	36.84	23

Table 11. Batch size comparison is conducted for MLLMs across a randomly sampled subset of 625 images (one image per class) by sending batches of 1, 5, and 10 images in a single request. For Qwen3-VL and GPT-4o, the results remain consistent across all batch sizes, with only negligible variation. In contrast, LLaVA-OV shows a significant decrease in accuracy as the batch size increases. Since the differences are minor for Qwen3-VL and GPT-4o and larger batches are more resource-efficient, a batch size of 10 is selected for the experiments. In contrast, LLaVA-OV is evaluated using a batch size of 1 in all experiments.

Model	In-Batch Ordering	ImGT	ReGT	OOP
		A ₆₂₅₀	A ₆₂₅₀	
Qwen3-VL	Random	63.47	70.83	734
	Same-Class	76.96	78.19	470
GPT-4o	Random	75.78	80.82	324
	Same-Class	86.03	84.61	155

Table 12. We evaluated the effect of in-batch ordering by comparing random class mixtures with batches containing images from the same ImGT class across a randomly sampled subset of 6250 images (10 images per class). Grouping images by class leads MLLMs to frequently assign the same label to all images within a batch, thereby increasing ImGT accuracy and alignment with the reannotated labels ReGT. Random ordering mitigates this batch-class bias. Therefore, random in-batch ordering is used in all experiments for models that process batches of images per request.

B.5. Preliminary experiments

Research on image classification with MLLMs remains limited, with only three methodologies proposed in the literature, corresponding to OW, MC, and CW tasks. There is little guidance on how to properly configure MLLMs for such evaluations, and no prior studies have systematically examined the impact of different parameter settings. Therefore, we present an ablation study on the parameters influencing image classification using MLLMs.

Batch size. We evaluate different batch sizes by sending batches of 1, 5, and 10 images per request to the LLaVA-OV, Qwen3-VL, and GPT-4o models. We do not perform this evaluation for InternVL3.5, as it only accepts a single image per request. The results in Tab. 11 show that Qwen3-VL and GPT-4o maintain nearly identical accuracy across all batch sizes, whereas LLaVA-OV experiences a dramatic drop in accuracy with larger batch sizes. Since batch size 10 provides stable results for both GPT-4o and Qwen3-VL and is more resource-efficient, we select it for all remaining experiments. In contrast, LLaVA-OV is evaluated using batch size 1, as it would be unfair to assess it under conditions known to reduce its performance.

Effect of image position within a batch on accuracy.

The impact of image position within a batch is presented in Tab. 13. Qwen3-VL and GPT-4o consistently maintain high accuracy regardless of image order, while LLaVA-OV experiences a significant drop in performance for images appearing later in the batch, consistent with its sensitivity to larger batch sizes.

		ImGT		ReGT	
Img Pos.	Batch	$A_{63(62)}$		$A_{63(62)}$	OOP
LLaVA-OV	1	1	44.44	60.32	18
	1	5	42.86 -1.6	58.73 -1.6	20 +2
	1	10	33.33 -11.1	52.38 -7.9	23 +5
	5	1	55.56	69.84	11
	5	5	26.98 -28.6	34.92 -34.9	28 +17
	5	10	31.75 -23.8	39.68 -30.2	25 +14
	10	1	37.10	50.00	22
	10	5	16.13 -21.0	29.03 -21.0	38 +16
	10	10	17.74 -19.4	30.65 -19.4	33 +11
Qwen3-VL	1	1	63.49	73.02	1
	1	5	66.67 +3.2	76.19 +3.2	2 +1
	1	10	66.67 +3.2	76.19 +3.2	2 +1
	5	1	71.43	85.71	0
	5	5	68.25 -3.2	80.95 -4.8	5 +5
	5	10	66.67 -4.8	77.78 -7.9	5 +5
	10	1	61.29	72.58	7
	10	5	53.23 -8.1	69.35 -3.2	8 +1
	10	10	56.45 -4.8	70.97 -1.6	9 +2
GPT-4o	1	1	69.84	79.37	2
	1	5	73.02 +3.2	82.54 +3.2	2
	1	10	69.84	79.37	1 -1
	5	1	76.19	88.89	1
	5	5	74.60 -1.6	88.89	3 +2
	5	10	74.60 -1.6	85.71 -3.2	2 +1
	10	1	70.97	83.87	4
	10	5	70.97	85.48 +1.6	3 -1
	10	10	80.65 +9.7	90.32 +6.5	3 -1

Table 13. The 1st, 5th, and 10th images from each set of requests with batch sizes 1, 5, and 10 were selected, and their accuracies were computed. Original requests were performed across a randomly sampled subset of 625 images (one image per class). The image positions vary depending on the batch size: in batch size 1, the image is always first; in batch size 5, the 1st image is first while the 5th and 10th are last; and in batch size 10, the 1st image is first, the 5th is in the middle, and the 10th is last. The results show that Qwen3-VL and GPT-4o maintain nearly stable accuracy regardless of image position, with only small deviations. In contrast, LLaVA-OV exhibits a noticeable decrease in accuracy for images appearing later in the batch, consistent with its sensitivity to larger batch sizes (see Tab. 11).

Batch composition bias. Using this fixed batch size for Qwen3-VL and GPT-4o, we evaluate the effect of in-batch image ordering on model behavior. We compare randomly mixed batches with batches containing only images from the same ImGT class. As shown in Tab. 12, class-grouped batches frequently cause both MLLMs to assign the same label to every image, inflating ImGT and ReGT accuracy.

Random ordering mitigates this batch-class bias; therefore, we adopt random ordering for all experiments with these models.

Class names or class IDs? With batch size and ordering fixed, we compare two response formats: requiring the models to output a class ID from a provided mapping or directly output a Class Name from the supplied list. As shown in Tab. 14, GPT-4o performs similarly in both settings, although the Class Name format occasionally produces out-of-prompt (OOP) outputs that can later be leveraged in the CW+ experiment. For LLaVA-OV, InternVL3.5, and Qwen3-VL, the Class Name format yields noticeably higher accuracy compared to the ID format, while still providing OOP predictions. Therefore, we use the Class Name format in all experiments.

Comparison of language-models (LMs) for prediction mapping. We evaluate different LMs for our OW setup: (i) Sentence-BERT [31], which is optimized for general-purpose sentence-level semantic similarity and provides embeddings aligned for textual comparison (following a similar approach to our OW semantic-similarity baseline in Conti et al. [7]); (ii) SigLIP 2 [35], a state-of-the-art language model designed to produce high-quality, image-grounded text embeddings; and (iii) the newly released Qwen3 text encoder [41], tailored for multimodal models and naturally integrated with the Qwen3-VL architecture. The results are presented in Tab. 18. Templating improves performance for all encoders.

PaliGemma 2 and GPT-4o perform best when paired with the SigLIP 2, while LLaVA-OV, InternVL3.5 and Qwen3-VL achieve the highest performance with Qwen3-Embedding-8B. The model-specific LM selected based on OW accuracy is used for evaluation in both the OW and CW+ setups in the main paper.

Distractor choice in the MC setup We explore several methods for the informed selection of challenging distractors for a class c in the 4-choice MC setup: (i) using the confusion matrix of the EVA-02 model, and (ii) selecting classes closest to c in the BERT embedding space, similar to Liu et al. [21]. The results are shown in Tab. 19.

The BERT-based method can yield highly challenging distractors (*e.g.* distractors for “computer keyboard” include “typewriter keyboard”, “keyboard space bar”, and “laptop computer”), but it may also produce distractors that are no more difficult than random choices (*e.g.* the nearest classes to “lens cap” are “swimming cap”, “bottle cap”, and “shower cap”). Overall, BERT-based distractors are more challenging than completely random selection, yet remain less difficult than those derived from the EVA-02 confusion matrix.

Model	Response	ImGT			ReGT					
		A ₆₂₅	A ₆₂₅	S ₃₅₂	S ₊₃₁₆	S ₋₃₆	M ₂₄₀	M ₊₂₂₁	M ₋₁₉	OOP
LLaVA-OV	ID	7.68	14.24	9.38	9.81	5.56	9.58	9.95	5.26	0
	Class name	42.56 +34.9	52.00 +37.8	46.31	48.10	30.56	53.75	55.20	36.84	168
InternVL3.5	ID	57.60	67.20	62.22	64.24	44.44	70.00	72.85	36.84	6
	Class name	63.68 +6.1	72.96 +5.8	67.05	69.30	47.22	77.92	80.54	47.37	6
Qwen3-VL	ID	48.00	57.28	54.55	56.96	33.33	55.42	58.37	21.05	0
	Class name	64.16 +16.2	72.16 +14.9	71.88	75.95	36.11	68.75	72.40	26.32	61
GPT-4o	ID	70.24	78.08	75.00	79.43	36.11	79.58	83.26	36.84	0
	Class name	74.24 +4.0	81.92 +3.8	80.68	85.44	38.89	81.25	85.07	36.84	23

Table 14. We compare two response formats for MLLMs across a randomly sampled subset of 625 images (one image per class): *ID*, where the model outputs a class ID using a provided ID–class name mapping (e.g. 0 – “tench”, ...), and *Class Name*, where the model directly selects a class name from the supplied list. Although the **accuracy deltas relative to the ID format** vary substantially across models, the Class Name setup yields higher accuracy for all models. Moreover, this setting occasionally produces out-of-prompt (OOP) outputs, which can later be leveraged in the CW+ setup. Therefore, the Class Name setup is used in all experiments.

For example, in the pure ImGT with distractors setup (commonly used as a baseline for MLLMs image recognition evaluation), the performance of GPT-4o on ImGT decreases nearly twice as much with EVA-02 distractors as with BERT-based ones (90.66% and 95.86% accuracy on ImGT, respectively), compared to random distractors (99.62% on ImGT).

C. Additional Results

C.1. Detailed overview of the OOP predictions

We present the distribution of out-of-prompt MLLMs predictions under the CW setup across four types in Tab. 16. We also report the exact number of OOP predictions for each label category, along with the number correctly mapped (using the best model-specific LM) in the CW+ setup, in Tab. 15. Predictions in category N do not require mapping, as any prediction for images in this category is considered correct in our setup.

C.2. Model comparison: Correlation of recall and correctness patterns

To analyze similarity in model behavior, we compute two complementary correlation measures, corresponding to the two panels in Fig. 9.

Per-class recall correlation (left). For each model, we compute per-class recall independently for every class represented in the reannotated image subset, restricting the analysis to single-label images only. Although the subset was reannotated for 625 classes, the images within it span 665 ImageNet-1k classes. We then calculate the Spearman correlation between these per-class recall vectors across

models. This correlation matrix captures similarity in class-wise error patterns rather than raw accuracy.

A clear structure emerges according to the training paradigm. Supervised models (EfficientNetV2, EfficientNet-L2, EVA-02) and the k -NN variant of DINOv3 form a tight, highly correlated cluster. VLMs: DINOv3 (dino.txt), SigLIP, and SigLIP 2 are strongly aligned with each other and moderately correlated with supervised models. In contrast, MLLMs exhibit lower similarity to traditional vision models, indicating that their failure modes differ substantially from both supervised and self-supervised approaches. We also compute per-class recall by treating the ground-truth ImGT labels as predictions. Notably, this vector shows strong alignment with high-capacity supervised and self-supervised models.

Image-level correctness correlation (right). In addition, we construct, for each model, a binary image-level correctness vector over all images with valid label(s) in the reannotated set, where each entry indicates whether the model prediction is correct. We then compute pairwise similarity between these binary vectors using the Phi coefficient. Unlike the left panel, this analysis operates at the image level and includes multi-label cases. The resulting matrix reflects agreement on which specific images are classified correctly or incorrectly. While the results differ slightly from the left panel, they still highlight the MLLMs cluster, which is weakly correlated with supervised and self-supervised models.

C.3. Stability under repeated evaluation

The results of accuracy deviation are presented in Tab. 17. With the temperature set to 0, GPT-4o exhibits non-zero

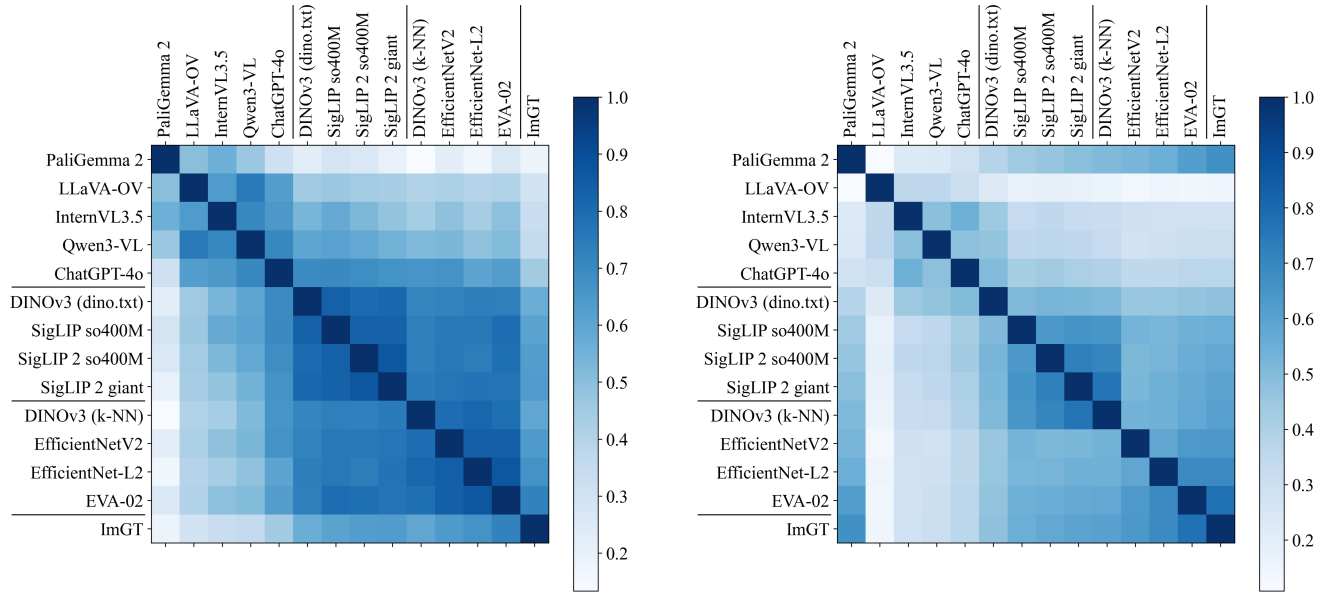


Figure 9. Correlation matrices across models evaluated on reannotated labels (ReGT). **Left:** Computes per-class recall for single-label images only and measures cross-model similarity using Spearman correlation. **Right:** Builds an image correctness vector including all images with valid label(s) and computes cross-model similarity using the Phi coefficient. The blocks indicate MLLMs, VLMs, supervised models and original ground-truth (ImGT).

variability, whereas LLaVA-OV, InternVL3.5, and Qwen3-VL behave deterministically.



620 - laptop computer



681 - notebook computer



836 - sunglass



837 - sunglasses

In the modern context, these terms effectively mean the same thing. Distinguishing between them solely from visual features is close to impossible. The image content of the classes is the same.

Sunglass is defined as “a convex lens that focuses the rays of the sun; used to start a fire” in WordNet, the difference was lost in the original annotation process. The image content of the classes is the same.



742 - printer



713 - photocopier



975 - lakeshore



978 - seashore

Printers and photocopiers used to be separate devices, but there are also multi-functional ones. Distinguishing them visually is difficult, and in modern context, stand-alone photocopiers are no longer commonly used.

It's difficult to identify whether the water comes from ocean, sea, lake or river, unless it is a well-known geographical location or a characteristic wildlife can be observed.



638 - tights/leotard



639 - bathing suit



454 - bookstore



624 - library

The original meaning of the first term was lost during annotation, similar to what happened with “sunglass”. As a result, the image content of the classes is now indistinguishable based on visual features.

It is challenging to distinguish a bookstore from a library solely from an interior view, unless a distinguishing object like a cash register is visible. This leaves room for ambiguity and speculation.

Figure 10. Class pairs (part 1/2) considered equivalent during evaluation (*i.e.* for a pair of classes $\{c_1, c_2\}$ and an image labeled c_1 , a predicted label c_2 is also considered correct). Each pair is accompanied by a brief note explaining the decision.



657 - missile



744 - projectile, missile



461 - breastplate



524 - cuirass

The image content of the classes is mostly the same: the majority of the images are missiles.

Breastplate only provides front coverage, while a cuirass covers the whole body. They share the same visual features from the front view, which is the predominant one.



435 - bathtub



876 - tub, vat



248 - Eskimo dog



250 - Siberian Husky

The image content of the classes is mostly the same.

The majority of the "Eskimo dog" class are huskies.



482 - cassette player



848 - tape player



899 - water jug



725 - drink pitcher

Distinguishing between a cassette player and tape player from images is often unreliable. The terms are commonly used interchangeably, as the visual differences are minimal.

Both classes represent containers for pouring liquids with identical structures; it is hard to tell when a water jug becomes a pitcher and vice versa.

Figure 11. Class pairs (part 2/2) considered equivalent during evaluation (*i.e.* for a pair of classes $\{c_1, c_2\}$ and an image labeled c_1 , a predicted label c_2 is also considered correct). Each pair is accompanied by a brief note explaining the decision.

		OOP		Correctly Mapped	
		#	%	#	%
InternVL3.5	A ₃₁₂₅₀	271	0.87	83	30.63
	S ₁₈₀₇₁	145	0.80	34	23.45
	S+ ₁₆₁₇₇	130	0.80	34	26.15
	S- ₁₈₉₄	15	0.79	0	0.00
	M ₁₁₈₃₄	92	0.78	15	16.30
	M+ ₁₀₇₅₆	79	0.73	12	15.19
	M- ₁₀₇₈	13	1.21	3	23.08
	N ₁₃₄₅	34	2.53	-	-
GPT-4o	A ₃₁₂₅₀	1647	5.27	554	33.64
	S ₁₈₀₇₁	717	3.97	142	19.80
	S+ ₁₆₁₇₇	553	3.42	119	21.52
	S- ₁₈₉₄	164	8.66	23	14.02
	M ₁₁₈₃₄	710	6.00	192	27.04
	M+ ₁₀₇₅₆	603	5.61	177	29.35
	M- ₁₀₇₈	107	9.93	15	14.02
	N ₁₃₄₅	220	16.36	-	-
Qwen3-VL	A ₃₁₂₅₀	3290	10.53	1275	38.75
	S ₁₈₀₇₁	1671	9.25	497	29.74
	S+ ₁₆₁₇₇	1410	8.72	456	32.34
	S- ₁₈₉₄	261	13.78	41	15.71
	M ₁₁₈₃₄	1294	10.93	453	35.01
	M+ ₁₀₇₅₆	1135	10.55	421	37.09
	M- ₁₀₇₈	159	14.75	32	20.13
	N ₁₃₄₅	325	24.16	-	-
LLaVA-OV	A ₃₁₂₅₀	8364	26.76	3720	44.48
	S ₁₈₀₇₁	4355	24.10	1797	41.26
	S+ ₁₆₁₇₇	3823	23.63	1679	43.92
	S- ₁₈₉₄	532	28.09	118	22.18
	M ₁₁₈₃₄	3437	29.04	1351	39.31
	M+ ₁₀₇₅₆	3101	28.83	1282	41.34
	M- ₁₀₇₈	336	31.17	69	20.54
	N ₁₃₄₅	572	42.53	-	-

Table 15. Overview of MLLMs out-of-prompt across label categories. Counts (#) indicate predictions falling outside the provided class names in the CW setup and the number correctly mapped (#) in CW+. Harder label categories: M- and S-, which do not contain the ImGT label, and N, which contains no label at all – exhibit a higher ratio of OOP predictions.

Model	Partial	IN	Abstain	Wrong
InternVL3.5	21.77	0.0	1.11	77.12
GPT-4o	35.34	3.22	6.38	55.07
Qwen3-VL	26.81	1.67	0.0	71.52
LLaVA-OV	36.29	2.59	0.04	61.08

Table 16. Distribution of out-of-prompt MLLMs predictions. “Partial” denotes cases where the predicted string is a subset of any of the provided class names, regardless of word order. “IN” corresponds to predictions that exactly match the commonly used OpenAI ImageNet-1k class names. “Abstain” refers to predictions in the form of “I don’t know” or similar expressions (including LLM-generated variations). “Wrong” includes all remaining predictions.

Model	Batch	ImGT			ReGT					OOP
		A ₆₂₅	A ₆₂₅	S ₃₅₂	S ₊₃₁₆	S ₋₃₆	M ₂₄₀	M ₊₂₂₁	M ₋₁₉	
GPT-4o	10	74.69 ±0.19	81.32 ±0.18	79.87 ±0.19	84.49 ±0.21	39.25 ±0.82	80.89 ±0.35	84.72 ±0.36	36.33 ±0.58	30.13 ±1.11

Table 17. Accuracy deviation observed over 31 repeated evaluations of the same 625-image subset using the GPT-4o model with temperature set to 0. Despite these deterministic settings, the model exhibits small but non-zero variability, reflected in the 95% confidence intervals, which may cause slight differences when replicating the experiments. LLaVA-OV, InternVL3.5, and Qwen3-VL are fully deterministic and are therefore not included in this table.

Emb. Space	ImGT		ReGT						
	A ₃₁₂₅₀	A ₃₁₂₅₀	S ₁₈₀₇₁	S ₊₁₆₁₇₇	S ₋₁₈₉₄	M ₁₁₈₃₄	M ₊₁₀₇₅₆	M ₋₁₀₇₈	
PaliGemma 2	Sentnce-BERT	30.60	41.41	32.58	34.01	20.38	48.24	49.58	34.88
	Sentence-BERT [†]	31.89	42.81	33.86	35.32	21.44	49.98	51.33	36.55
	Qwen3-Embedding-8B	33.24	43.53	35.49	37.05	22.23	49.37	50.99	33.21
	Qwen3-Embedding-8B [†]	36.52	47.51	39.05	40.71	24.92	54.45	56.16	37.38
	SigLIP 2	34.56	45.04	36.45	38.23	21.28	51.90	53.51	35.81
	SigLIP 2 [†]	37.11	47.94	39.74	41.49	24.76	54.55	56.24	37.66
LLaVA-OV	Sentence-Bert	55.72	64.56	61.13	64.42	33.05	65.76	68.60	37.38
	Sentence-BERT [†]	56.57	65.60	61.76	65.03	33.84	67.54	70.43	38.78
	Qwen3-Embedding-8B	57.56	65.71	62.22	65.42	34.90	67.14	70.22	36.36
	Qwen3-Embedding-8B [†]	62.00	70.58	67.11	70.67	36.69	72.52	75.87	39.05
	SigLIP 2	59.40	67.24	64.58	68.12	34.42	67.57	70.59	37.38
	SigLIP 2 [†]	61.98	70.35	67.38	70.84	37.91	71.50	74.67	39.89
InternVL3.5	Sentnce-BERT	51.94	61.15	55.51	58.48	30.15	65.33	68.34	35.25
	Sentence-SBERT [†]	53.11	62.63	56.75	59.71	31.47	67.36	70.30	38.03
	Qwen3-Embedding-8B	53.72	62.07	56.54	59.51	31.20	66.21	69.20	36.36
	Qwen3-Embedding-8B [†]	59.23	68.18	62.44	65.78	33.90	73.33	76.66	40.07
	SigLIP 2	55.25	63.09	58.67	61.85	31.47	65.65	68.70	35.25
	SigLIP 2 [†]	58.91	67.16	62.53	65.76	34.90	70.51	73.72	38.50
Qwen3-VL	Sentence-BERT	57.65	66.51	62.72	66.22	32.84	68.49	71.46	38.87
	Sentence-BERT [†]	60.35	69.21	65.41	69.05	34.32	71.51	74.65	40.26
	Qwen3-Embedding-8B	59.28	66.89	62.45	65.96	32.42	69.90	73.21	36.83
	Qwen3-Embedding-8B [†]	68.74	76.68	73.61	77.79	37.91	78.71	82.46	41.28
	SigLIP 2	59.27	65.66	63.86	67.96	28.83	64.50	67.83	31.26
	SigLIP 2 [†]	65.82	73.07	71.23	75.40	35.59	72.82	76.40	37.01
GPT-4o	Sentence-BERT	64.14	71.49	70.22	74.57	33.05	70.20	73.77	34.51
	Sentence-BERT [†]	64.84	72.58	71.03	75.28	34.69	71.83	75.51	35.06
	Qwen3-Embedding-8B	63.91	70.59	68.62	72.72	33.63	70.25	74.00	32.84
	Qwen3-Embedding-8B [†]	70.32	77.29	75.61	80.23	36.22	77.28	81.41	36.09
	SigLIP 2 ViT-gopt-384	67.42	73.94	73.11	77.41	36.38	72.26	76.20	32.93
	SigLIP 2 [†] ViT-gopt-384	70.92	77.58	76.59	81.08	38.23	76.55	80.75	34.69

Table 18. Results for the OW setup with different language models (LMs) used for prediction mapping are reported. † denotes the use of templating following Radford et al. [29]. Sentence-BERT is included, as it is used for semantic similarity in Conti et al. [7]. Templating improves performance for all LMs. SigLIP 2 encoding performs best for PaliGemma 2 and GPT-4o, while Qwen3-Embedding-8B encoding achieves the highest performance for LLaVA-OV, InternVL3.5, and Qwen3-VL. The model-specific LM selected based on OW accuracy is used for evaluation in both the OW and CW+ setups in the main paper.

Distractors	ImGT			ReGT					
	A ₆₂₅	A ₆₂₅	S ₃₅₂	S+ ₃₁₆	S- ₃₆	M ₂₄₀	M+ ₂₂₁	M- ₁₉	
LLaVA-OV	ImGT + random	99.28 ±0.15	90.75 ±0.11	89.36 ±0.13	99.52 ±0.14	0.18 ±0.25	91.52 ±0.18	99.39 ±0.20	0.00 ±0.00
	ImGT + confEVA (ImGT)	79.93 ±0.32	76.02 ±0.30	73.13 ±0.45	81.46 ±0.50	0.00 ±0.00	76.96 ±0.47	83.58 ±0.51	0.00 ±0.00
	ImGT + confBERT (ImGT)	88.59 ±0.29	82.65 ±0.26	79.66 ±0.42	88.73 ±0.46	0.00 ±0.00	84.65 ±0.32	91.93 ±0.35	0.00 ±0.00
	ReGT + confEVA (ReGT)	44.28 ±0.26	78.36 ±0.39	81.42 ±0.43	81.49 ±0.48	80.83 ±1.40	70.90 ±0.69	71.77 ±0.64	60.78 ±3.86
	ReGT + confBERT (ReGT)	49.19 ±0.25	84.92 ±0.42	89.08 ±0.42	89.21 ±0.47	87.99 ±1.24	76.75 ±0.82	76.57 ±0.91	78.78 ±2.66
	ImGT + ReGT + random	89.99 ±0.28	95.21 ±0.17	95.44 ±0.21	99.55 ±0.14	59.32 ±1.38	94.22 ±0.27	99.71 ±0.16	30.39 ±2.89
	ImGT + ReGT + confEVA (ImGT, ReGT)	82.17 ±0.31	90.01 ±0.20	87.78 ±0.23	90.74 ±0.25	61.74 ±1.08	91.92 ±0.31	97.23 ±0.25	30.22 ±2.95
	ImGT + 999 (Closed World (CW))	42.56 ±0.00	52.00 ±0.00	46.31 ±0.00	48.10 ±0.00	30.56 ±0.00	53.75 ±0.00	55.20 ±0.00	36.84 ±0.00
InternVL3.5	ImGT + random	99.64 ±0.11	90.97 ±0.08	89.54 ±0.10	99.72 ±0.11	0.18 ±0.25	91.83 ±0.13	99.72 ±0.14	0.00 ±0.00
	ImGT + confEVA (ImGT)	83.72 ±0.30	78.95 ±0.24	76.04 ±0.34	84.71 ±0.38	0.00 ±0.00	80.31 ±0.40	87.21 ±0.44	0.00 ±0.00
	ImGT + confBERT (ImGT)	92.68 ±0.22	85.42 ±0.18	82.64 ±0.26	92.06 ±0.29	0.00 ±0.00	87.50 ±0.28	95.02 ±0.30	0.00 ±0.00
	ReGT + confEVA (ReGT)	46.49 ±0.19	82.83 ±0.37	84.41 ±0.33	84.71 ±0.38	81.81 ±0.82	78.14 ±0.75	79.10 ±0.65	67.06 ±3.56
	ReGT + confBERT (ReGT)	51.32 ±0.19	88.97 ±0.24	91.84 ±0.26	92.06 ±0.29	89.88 ±0.62	83.24 ±0.54	83.35 ±0.53	82.00 ±2.58
	ImGT + ReGT + random	91.98 ±0.22	94.90 ±0.15	94.99 ±0.16	99.72 ±0.11	53.41 ±1.20	94.07 ±0.30	99.83 ±0.10	27.17 ±3.60
	ImGT + ReGT + confEVA (ImGT, ReGT)	85.89 ±0.29	90.53 ±0.24	88.78 ±0.38	92.86 ±0.36	52.96 ±1.76	91.79 ±0.36	97.35 ±0.23	27.17 ±2.91
	ImGT + 999 (Closed World (CW))	63.68 ±0.00	72.96 ±0.00	67.05 ±0.00	69.30 ±0.00	47.22 ±0.00	77.92 ±0.00	80.54 ±0.00	47.37 ±0.00
Qwen3-VL	ImGT + random	99.34 ±0.09	90.67 ±0.08	89.41 ±0.08	99.59 ±0.09	0.09 ±0.18	91.22 ±0.17	99.07 ±0.18	0.00 ±0.00
	ImGT + confEVA (ImGT)	85.80 ±0.29	80.74 ±0.26	77.67 ±0.27	86.52 ±0.31	0.00 ±0.00	82.59 ±0.42	89.70 ±0.46	0.00 ±0.00
	ImGT + confBERT (ImGT)	93.13 ±0.22	86.54 ±0.17	84.41 ±0.27	94.03 ±0.30	0.00 ±0.00	87.81 ±0.23	95.36 ±0.25	0.00 ±0.00
	ReGT + confEVA (ReGT)	47.14 ±0.17	82.01 ±0.36	86.40 ±0.30	86.52 ±0.31	85.39 ±1.26	73.09 ±0.77	73.92 ±0.67	63.50 ±3.69
	ReGT + confBERT (ReGT)	51.88 ±0.18	88.57 ±0.34	93.70 ±0.32	94.03 ±0.30	90.77 ±1.13	79.48 ±0.66	79.39 ±0.64	80.47 ±2.78
	ImGT + ReGT + random	91.95 ±0.25	94.23 ±0.11	94.12 ±0.14	99.59 ±0.09	46.06 ±1.46	93.60 ±0.21	99.64 ±0.11	23.43 ±2.48
	ImGT + ReGT + confEVA (ImGT, ReGT)	86.32 ±0.26	90.77 ±0.21	89.14 ±0.27	93.86 ±0.28	47.67 ±1.18	91.88 ±0.28	97.65 ±0.28	24.79 ±2.55
	ImGT + 999 (Closed World (CW))	64.16 ±0.00	72.16 ±0.00	71.88 ±0.00	75.95 ±0.00	36.11 ±0.00	68.75 ±0.00	72.40 ±0.00	26.32 ±0.00
GPT-4o	ImGT + random	99.62 ±0.07	90.95 ±0.05	89.49 ±0.07	99.67 ±0.07	0.09 ±0.18	91.85 ±0.10	99.75 ±0.11	0.00 ±0.00
	ImGT + confEVA (ImGT)	90.66 ±0.22	85.12 ±0.21	84.27 ±0.26	93.87 ±0.29	0.00 ±0.00	84.31 ±0.39	91.56 ±0.42	0.00 ±0.00
	ImGT + confBERT (ImGT)	95.86 ±0.17	88.76 ±0.12	87.71 ±0.19	97.70 ±0.21	0.00 ±0.00	88.75 ±0.18	96.38 ±0.20	0.00 ±0.00
	ReGT + confEVA (ReGT)	51.35 ±0.21	84.26 ±0.37	92.45 ±0.36	93.90 ±0.31	79.66 ±1.50	70.09 ±0.89	70.78 ±0.83	62.14 ±3.36
	ReGT + confBERT (ReGT)	54.10 ±0.12	89.37 ±0.35	96.72 ±0.23	97.75 ±0.20	87.63 ±1.11	77.14 ±0.76	76.91 ±0.77	79.80 ±2.69
	ImGT + ReGT + random	91.77 ±0.26	94.89 ±0.13	94.79 ±0.16	99.67 ±0.07	51.97 ±1.35	94.31 ±0.27	99.80 ±0.09	30.56 ±2.97
	ImGT + ReGT + confEVA (ImGT, ReGT)	88.31 ±0.29	92.52 ±0.15	91.59 ±0.20	96.36 ±0.15	49.73 ±1.27	92.86 ±0.31	98.16 ±0.20	31.24 ±3.30
	ImGT + 999 (Closed World (CW))	74.69 ±0.19	81.32 ±0.18	79.87 ±0.19	84.49 ±0.21	39.25 ±0.82	80.89 ±0.35	84.72 ±0.36	36.33 ±0.58

Table 19. 4-way multiple-choice (MC) results across a randomly sampled subset of 625 images (one image per class), reported with 95 % confidence intervals (CI). `confEVA()` and `confBERT()` denote functions that return challenging distractors based on the confusion matrix of EVA-02 and the distance between class names in the BERT embedding space, respectively. The Closed World result corresponds to using 999 distractors.

GPT-4o Prompt

You are an image classifier.

You will receive up to 50 images in order (image "1" = first, "2" = second, etc.).

You are also provided with a list of class names: {class_list}.

Classification Rules:

- For each image, return the single class name that best represents the main subject of the image.
- Choose only one class per image - the most relevant or dominant one.
- Only return classes from the provided list.

Output Rules:

- Return exactly one output per image.
 - Each output must be only a single class name (no separators or lists).
 - Do not include explanations, confidence scores, or extra text.
-

LLaVA-OV & InternVL3.5 & Qwen3-VL Prompt

You are an image classifier.

You will receive up to 50 images in order (image "1" = first, "2" = second, etc.).

You are also provided with a list of class names: {class_list}.

Your output will be automatically structured as JSON with keys "1", "2", "3", etc. corresponding to the order of images in the request.

Each value should be the predicted class name for that image.

Classification Rules:

- For each image, return the class name only from the provided list.
- Only return classes from the provided list.

Output Rules:

- Return exactly one JSON key per image ("1", "2", "3", etc.).
 - Each value must be only class names.
 - Do not include explanations, confidence scores, or extra text.
-

Table 20. Prompts for the Closed World setup. The top panel shows the prompt for the GPT-4o model, while the bottom panel shows the corresponding prompt for the LLaVA-OV, InternVL3.5 and Qwen3-VL models.

GPT-4o Prompt

You are an open-set fine-grained image classifier.

You will receive up to 50 images in order (image "1" = first, "2" = second, etc.).

Classification Rules:

- For each image, identify the dominant object.
- Return the most fine-grained, specific label that accurately describes that object (e.g., "golden retriever puppy", "1950s red convertible", "blue morpho butterfly", "ceramic coffee mug with floral pattern").
- Use natural-language labels that reflect detailed visual distinctions such as species, make/model, style, color, or material.
- Avoid generic terms like "dog", "car", or "bird" when a more specific subtype or description is visually inferable.
- If the dominant object cannot be clearly identified, return a concise descriptive label of its appearance (e.g., "abstract metal sculpture", "blurry human silhouette").
- Focus only on the dominant object, even if multiple are present.

Output Rules:

- Return exactly one output per image.
 - The output must contain only the final label (no punctuation beyond normal text, no explanations, confidence scores, or extra text).
-

LLaVA-OV & InternVL3.5 & Qwen3-VL Prompt

You are an open-set fine-grained image classifier.

You will receive up to 50 images in order (image "1" = first, "2" = second, etc.).

Your output will be automatically structured as JSON with keys "1", "2", "3", etc. corresponding to the order of images in the request.

Each value should be the predicted label for that image.

Classification Rules:

- For each image, identify the dominant object.
- Return the most fine-grained, specific label that accurately describes that object (e.g., "golden retriever puppy", "1950s red convertible", "blue morpho butterfly", "ceramic coffee mug with floral pattern").
- Use natural-language labels that reflect detailed visual distinctions such as species, make/model, style, color, or material.
- Avoid generic terms like "dog", "car", or "bird" when a more specific subtype or description is visually inferable.
- If the dominant object cannot be clearly identified, return a concise descriptive label of its appearance (e.g., "abstract metal sculpture", "blurry human silhouette").
- Focus only on the dominant object, even if multiple are present.

Output Rules:

- Return exactly one output per image.
 - The output must contain only the final label (no punctuation beyond normal text, no explanations, confidence scores, or extra text).
-

Table 21. Prompts for the Open World setup. The top panel shows the prompt for the GPT-4o model, while the bottom panel shows the corresponding prompt for the LLaVA-OV, InternVL3.5 and Qwen3-VL models.

LLaVA-OV & InternVL3.5 & Qwen3-VL & GPT-4o Prompt

You are an image classifier. You will receive one image. You are also provided with four multiple-choice options (A, B, C, D).

What is the main object in this image? {dynamic_choices}

Classification Rules:

- For the image, return the letter (A, B, C, or D) that corresponds to the correct option.
- Only return one letter.

Output Rules:

- Return exactly one letter (A, B, C, or D).
 - Do not include explanations, the class name, or extra text.
 - Your answer must be only the letter.
-

Table 22. Prompt for the Multiple-Choice setup. The same prompt is used for all MLLMs.